Resolving widespread incomplete and uneven archaeal classifications based on a rank-normalized genome-based taxonomy

Christian Rinke[1], Maria Chuvochina[1], Aaron J. Mussig[1], Pierre-Alain Chaumeil[1], Adrian A. Davin[1], David W. Waite[2], William B Whitman[3], Donovan H. Parks[1], Philip Hugenholtz[1]

[1] Australian Centre for Ecogenomics, School of Chemistry and Molecular Biosciences, The University of Queensland, Brisbane, Australia
[2] School of Biological Sciences, The University of Auckland, New Zealand
[3] Department of Microbiology, University of Georgia Athens, GA, USA

Abstract

An increasing wealth of genomic data from cultured and uncultured microorganisms provides the opportunity to develop a systematic taxonomy based on evolutionary relationships. Here we propose a standardized archaeal taxonomy, as part of the Genome Taxonomy Database (GTDB), derived from a 122 concatenated protein phylogeny that resolves polyphyletic groups and normalizes ranks based on relative evolutionary divergence (RED). The resulting archaeal taxonomy is stable under a range of phylogenetic variables, including marker genes, inference methods, corrections for rate heterogeneity and compositional bias, tree rooting scenarios, and expansion of the genome database. Rank normalization was shown to robustly correct for substitution rates varying up to 30-fold using simulated datasets. Taxonomic curation follows the rules of the International Code of Nomenclature of Prokaryotes (ICNP) while taking into account proposals to formally recognise the rank of phylum and to use genome sequences as type material. The taxonomy is based on 2,392 quality screened archaeal genomes, the great majority of which (93.3%) required one or more changes to their existing taxonomy, mostly as a result of incomplete classification. In total, 16 archaeal phyla are described, including reclassification of three major monophyletic units from the former Euryarchaeota and one phylum resulting from uniting the TACK superphylum into a single phylum. The taxonomy is publicly available at the GTDB website (https://gtdb.ecogenomic.org).

Main

Carl Woese's discovery of the Archaea in 1977, originally termed Archaebacteria (Woese and Fox, 1977) gave rise to the recognition of a new domain of life and fundamentally changed our view of cellular evolution

on Earth. In the following decades, an increasing number of archaea were described, initially from extreme environments but subsequently also from soils, oceans, freshwater, and animal guts, highlighting the global importance of this domain (Gribaldo and Brochier-Armanet, 2006). Since their recognition, archaea have been classified primarily via genotype, i.e. small subunit (SSU) rRNA gene sequences, and hence, compared to bacteria, they suffer less from historical misclassifications based on phenotypic properties (Zuo et al., 2015). Using the SSU rRNA gene, Woese initially described two major lines of archaeal descent, the Euryarchaeota and the Crenarchaeota (Woese et al., 1990), and in the following years all newly discovered archaeal lineages were added to these two main groups. Non-extremophilic Archaea were generally classified as Euryarchaeota (Spang et al., 2017), which together with the discovery of novel extremophile euryarchaeotes (Baker et al., 2020) contributed to a considerable expansion of this lineage. Eventually two new archaeal phyla were proposed based on phylogenetic novelty of their SSU rRNA sequences; the Korarchaeota (Barns et al., 1996), recovered from hot springs in Yellowstone National Park, and the nanosized, symbiotic Nanoarchaeota (Huber et al., 2002), co-cultured from a submarine hot vent. By the mid-2000s, archaeal classification had begun to leverage genome sequences and the first sequenced crenarchaeote, *Ca.* Cenarchaeum symbiosum from a marine sponge (Hallam et al., 2006), was used to argue that mesophilic archaea should be considered as a separate phylum from hyperthermophilic Crenarchaeota for which the name Thaumarchaeota was eventually proposed (Brochier-Armanet et al., 2008). Subsequently the field experienced a burst in availability of genomic data due to the substantial acceleration of culture-independent genome recovery driven by improvements in high throughput sequencing (Adam et al., 2017; Spang et al., 2017). This resulted in the description and naming of several new archaeal lineages, including the candidate phyla Aigarchaeota (Nunoura et al., 2011), Geoarchaeota (Kozubal et al., 2013) and Bathyarchaeota (Meng et al., 2014), previously reported as members of the Crenarchaeota based on SSU rRNA data. Some of the proposed phyla were met with criticism, such as the Geoarchaeota, which was considered to be a member of the order Thermoproteales rather than a novel phylum (Guy et al., 2014). All former crenarchaeal lineages (Adam et al., 2017) were then recombined into the TACK superphylum, originally comprising the Thaumarchaeota, Aigarchaeota, the remaining Crenarchaeota, and Korarchaeota (Guy and Ettema, 2011), and more recently the Verstraetearchaeota (Vanwonterghem et al., 2016).

New archaeal lineages were also described outside the Euryarchaeota and TACK, which were ultimately classified into two superphyla, DPANN and Asgard (Rinke et al., 2013; Zaremba-Niedzwiedzka et al., 2017). DPANN was originally proposed based on five phyla; Diapherotrites, Parvarchaeota, Aenigmarchaeota, Nanoarchaeota and Nanohaloarchaeota (Rinke et al., 2013), but now also includes the Micrarchaeota, Woesearchaeota, Pacearchaeota, Altiarchaeota and Huberarchaeota (Adam et al., 2017; Baker et al., 2010; Castelle et al., 2015; Probst et al., 2018, 2014). The Asgard archaea are notable for their inferred sister relationship to the eukaryotes and were originally proposed based on the phyla Lokiarchaeota, Thorarchaeota, Odinarchaeota and Heimdallarchaeota (Seitz et al., 2016; Spang et al., 2015; Zaremba-Niedzwiedzka et al., 2017), followed by the Helarchaeota (Seitz et al., 2019). The net result of these cumulative activities is that archaeal classification at higher ranks is currently very uneven. The Euryarchaeota absorbed novel lineages and grew into a phylogenetic behemoth, whereas the Crenarchaeota

were split into multiple subordinate taxa including several shallow lineages, such as Geoarchaeota, which despite their phylogenetic disproportion have been given the same rank of phylum. Attempts to rectify this taxonomic bias included a proposal to reclassify TACK as a single phylum termed Proteoarchaeota (Petitjean et al., 2014) and to introduce a new taxonomic rank above the class level which would generate several superclasses within the Euryarchaeota (Adam et al., 2017; Petitjean et al., 2015).

Most of this activity, i.e. the proposing and naming of new phyla, has occurred outside the International Code of Nomenclature of Prokaryotes (Parker et al., 2019) because the ICNP does not currently extend to uncultured microorganisms nor recognise the ranks of phylum and superphylum. However, proposals have been made to include the rank of phylum (Oren et al., 2015) and to allow gene sequences to serve as type material (Whitman, 2016), which have been increasingly adopted informally by the research community (Chuvochina et al., 2019). Currently, uncultured archaea and bacteria can be provisionally named using *Candidatus* status (Murray and Stackebrandt, 1995). However, these names have no formal standing in nomenclature, do not have priority, and often contradict the current ICNP rules or are otherwise problematic (Oren, 2017). The waters have been further muddied by the proposal of names for higher taxa without designation of lower ranks and type material, which leaves them without nomenclatural anchors and their circumscription subject to dispute if they become polyphyletic (Chuvochina et al., 2019). In addition to these higher level classification issues, the current archaeal taxonomy suffers from the same phylogenetic inconsistencies observed in the Bacteria, such as polyphyletic taxa (e.g. class Methanomicrobia; see below), but to a lesser degree than the Bacteria due to the early integration of phylogeny and the relatively small size of the archaeal dataset. More problematic is the widespread incomplete classification of environmental archaeal sequences in the NCBI taxonomy, which are often only assigned to a candidate phylum with no subordinate rank names. This high degree of incomplete classification is likely due to a natural hesitancy to create novel genera and intermediate taxa for groups lacking isolated representatives. Further, it is our opinion that the most useful biological classification should be based on an evolutionary framework, which takes into account differing rates of evolution such that ancestral taxa of a given rank co-existed in time (Parks et al., 2018). Currently, differences in evolutionary rates are not explicitly taken into account in the NCBI taxonomy.

For the domain Bacteria these long-standing taxonomic issues and inconsistencies were recently addressed by proposing a standardized taxonomy referred to as the Genome Taxonomy Database (GTDB; gtdb.ecogenomic.org). The GTDB normalizes rank assignments using relative evolutionary divergence (RED) in a genome phylogeny, which takes into account differing evolutionary rates, followed by an extensive automated and manual taxonomy curation process. This approach resulted in taxonomic changes to over half of the nearly 95,000 analyzed bacterial genomes (Parks et al., 2018) and has recently been extended to a complete classification from domain to species (Parks et al., 2019). Here we present the GTDB taxonomy for the domain Archaea (release R04-RS89), comprising 2,392 quality screened genomes from cultivated and uncultured organisms. This taxonomic release circumscribes 16 phyla, including three phyla from major monophyletic units of the Euryarchaeota, and one phylum resulting from the amalgamation of the TACK

110 superphylum. The archaeal GTDB taxonomy is publicly available at the Genome Taxonomy Database
111 website (https://gtdb.ecogenomic.org/).
112
113
114
115

116 Results

117 **Reference genome tree and initial decoration with the NCBI taxonomy**
118 The archaeal Genome Taxonomy Database (GTDB; 04-RS89) currently comprises 2392 quality-filtered
119 genomes obtained from RefSeq/GenBank release 89 (*see Methods*, (Haft et al., 2018). Genomes were
120 clustered into species units based on average nucleotide identity (ANI; *see Methods*), resulting in 1248
121 species (Parks et al., 2019). A representative sequence of each species, i.e. the genome of the type strain
122 or the highest quality genome of an uncultivated species, was then used for phylogenomic analyses (**Table**
123 **S1**). The protein sequences for up to 122 conserved single-copy ubiquitous archaeal genes were recovered
124 from each genome (Parks et al., 2017); **Table S2, Fig. S1**), aligned, concatenated into a supermatrix, and
125 trimmed to 5124 columns (*see Methods*). A reference tree (ar122.r89) was inferred using the C10 protein
126 mixture model with the posterior mean site frequency (PMSF) approximation (Wang et al., 2018) implemented
127 in IQ-TREE (Nguyen et al., 2015). The PMSF model is a faster approximation of finite mixture models, which
128 capture the heterogeneity in the amino acid substitution process between sites, and is able to mitigate long-
129 branch attraction artefacts (Wang et al., 2018). Additional trees were inferred from different alignments and
130 with alternative inference methods to assess the robustness of the GTDB taxonomy (*see below*). The
131 reference tree was initially decorated with taxon names obtained from the NCBI taxonomy (Federhen, 2012)
132 standardized to seven canonical ranks as previously described (Parks et al., 2018). Strikingly, many archaeal
133 genomes had no canonical rank information beyond their phylum affiliation (31.0%), which is partly offset by
134 the extensive use of names with no rank in the NCBI taxonomy (**Fig. S2a**). This was particularly apparent for
135 DPANN phyla, which almost entirely lack information in the family to class ranks (**Fig. S2b**).
136
137 **Removal of polyphyletic groups and rank normalization**
138 Approximately 10% of NCBI-defined taxa above the rank of species (26 of 252) could not be reproducibly
139 resolved as monophyletic or operationally monophyletic in the reference tree (the latter is defined as having
140 an F measure $\geq$0.95; Parks et al., 2018; **Table S3;** *see Methods*). These include the phyla Nanoarchaeota,
141 Aenigmarchaeota and Woesearchaeota, which were intermingled with each other and with unclassified
142 archaeal genomes (**Fig. S3**). Another prominent example is the class Methanomicrobia, which comprised
143 three orders in NCBI, two of which (Methanosarcinales and Methanocellales) were clearly separated from the
144 type order Methanomicrobiales (**Fig. S4.**). To resolve these cases, the lineage containing the nomenclature
145 type retained the name. Where possible, all other groups were renamed following the International Code of

146 Nomenclature of Prokaryotes **(**ICNP) and recent proposals to modify the Code (*see Methods*). For example,
147 the Methanomicrobia were resolved in GTDB by reserving the name for the lineage containing the type genus
148 of the type order of the class, i.e. *Methanomicrobium*, and by reclassifying the two remaining orders into their
149 own classes; Methanosarcinia class. nov. and Methanocellia class. nov. (**Fig. S4**). These and other ICNP-
150 based rules used to standardize the curation process above the rank of genus are summarized in a decision
151 tree (**Fig. S21, Suppl. Text**). When nomenclature types were not available at the genus and species level,
152 the existing names were retained as placeholders with alphabetical suffixes indicating polyphyly. For
153 example, the genus *Thermococcus* is polyphyletic because it also comprises species of the genus
154 *Pyrococcus.* This polyphyly was resolved by retaining the name for the monophyletic group containing the
155 type species, *Thermococcus celer,* and by assigning alphabetical suffixes to three basal groups comprising
156 other *Thermococcus* genomes (**Fig. S5**). Note that *Thermococcus chitonophagus* was transferred to
157 *Pyrococcus* according to the GTDB reclassification due to its proximity to the type species of this genus (**Fig.**
158 **S5**).
159
160 Taxonomic ranks were normalized using the relative evolutionary divergence (RED) metric. This method
161 linearly interpolates the inferred phylogenetic distances between the last common ancestor (set to RED=0)
162 and all extant taxa (RED=1) providing an approximation of relative time of divergence (Parks et al., 2018).
163 We tested the tolerance of the RED approach to increasing differences in substitution rates between lineages
164 using simulated datasets. The approach was robust to variable rates up to 30-fold different (**Suppl. Text**),
165 which is likely substantially higher than naturally occurring variation between prokaryotic taxa (Marin et al.,
166 2017). Rank distributions in the NCBI-decorated reference tree were extremely broad, highlighting severely
167 under- and over-classified outlier taxa (**Fig. 1a)**. Rank distributions were normalized (Parks et al., 2018) by
168 systematically reclassifying outliers either by re-assignment to a new rank with associated nomenclatural
169 changes for Latin names, or by moving names to new interior nodes in the tree (**Fig. 1b)**. This resulted in
170 large movements of the median RED values of the higher ranks (order and above) to produce a normalized
171 distribution (**Fig. 1b**). Over half (56.4%) of all archaeal NCBI taxon names had to be changed in the GTDB
172 taxonomy, with the largest percentage of changes occurring at the phylum level (76.6%) (**Fig. 1c**). Examples
173 of changes at lower ranks due to RED normalization include the genus *Methanobrevibacter*, which was
174 divided into five genus-level groups; *Methanobrevibacter* which includes the type species and four genera
175 with alphabetical suffixes (*Methanobrevibacter_A to Methanobrevibacter_D*; **Fig S6**). GTDB names were
176 assigned to nodes with high bootstrap support (bs 98.5% ± 5.0%) to ensure taxonomic stability with a small
177 number of exceptions (bs <90%) to preserve existing classifications (**Table S4**). Overall, 93.3% of the 2,239
178 archaeal genomes present in NCBI release 89 had one or more changes in their taxonomic assignments
179 (**Fig. 1c**).
180
181 **Robustness of proposed archaeal taxonomy**
182 We tested the robustness of the monophyly and rank normalization of the proposed taxonomy in relation to
183 a number of standard phylogenetic variables including marker genes, inference method, compositional bias,
184 fast evolving sites, increasing number of genomes and rooting of the tree. Comparing tree similarities

185 indicated that marker choice had a stronger influence on the tree topology than inference methods and
186 substitution models (**Fig. S7; Fig. S8)**. However, for all subsequent comparisons we focused on the
187 robustness of the taxonomy, not the overall consistency of tree topologies, as only a subset of interior nodes
188 (69.9%) in the reference tree were used for taxon classification (**Table S5**).
189
190 *Markers*
191 As expected, individual protein phylogenies of the 122 markers had lower phylogenetic resolution than the
192 reference tree, particularly at the higher ranks of class and phylum (**Fig S9a, b**). However, 78.5% of the GTDB
193 taxa with ≥2 representatives above the rank of species were still recovered as monophyletic groups in ≥50%
194 of single protein trees, and on average taxa were resolved as monophyletic in 74.1% of the single protein
195 trees (**Fig 9c, d**). We also compared the GTDB taxonomy to SSU rRNA gene trees, due to their historical
196 importance in defining archaeal taxa. However, this was complicated by the absence of this gene (>900 nt
197 after quality-trimming) in almost half of the species representatives (578/1248; 46.3%). The majority (94.1%)
198 of species representatives lacking SSU rRNA sequences were draft MAG assemblies (**Table S6**), which often
199 lack this gene due to the difficulties of correctly assembling and binning rRNA repeats in metagenomic
200 datasets (Parks et al., 2017; Sieber et al., 2018). Over 84% of the GTDB taxa with ≥2 SSU rRNA
201 representatives were operationally monophyletic in the SSU rRNA tree, with loss of monophyly most
202 pronounced in the higher ranks (**Fig. S10**) as seen for the single protein phylogenies. Three alternative
203 concatenated protein marker datasets were assessed; rp1 (16 ribosomal proteins, **Table S7** (Hug et al.,
204 2016), rp2 (23 ribosomal proteins, **Table S7**, (Rinke et al., 2013) and 53 recently proposed archaeal markers
205 (ar.53; **Table S8** (Dombrowski et al., 2020). The great majority (≥95%) of GTDB taxa above the rank of genus
206 with ≥2 representatives were recovered as monophyletic groups in the three alternative marker set trees
207 inferred using the same C10 PMSF mixture model as the reference tree (**Fig. 4; Fig. S11**) (Rinke et al., 2013).
208 The small percentage of taxa not resolved in the alternative trees (**Fig S11; Table S9**) were well supported
209 in the reference tree (average bootstrap support 90.3±8.8% ;**Fig. S12**). However, these taxa were resolved
210 as operationally monophyletic in a lower proportion of individual protein trees than other GTDB taxa
211 (33.7±14.7% vs 77.1±18.3% respectively). The RED distributions of the GTDB taxa were comparable in the
212 reference, rp1 and rp2 trees, whereas the SSU rRNA tree had a substantially broader distribution (**Fig. 2a,e,**
213 **Fig. S13**), likely reflecting undersampling of the topology, lower resolution of single marker genes relative to
214 concatenated marker sets and potentially compositional bias in the SSU rRNAs of thermophiles (Galtier &
215 Lobry, 1997).
216
217 *Inference methods and models*
218 We overlaid the IQ-TREE-based taxonomy onto trees inferred with different models (e.g. C20, C60; **Table**
219 **S10**) and phylogenetic inference tools, including FastTree and ExaML (maximum likelihood), PhyloBayes
220 (Bayesian), and ASTRAL (supertree). All methods were applied to the 122 archaeal marker set with the
221 exception of the ASTRAL supertree, which was also applied to a 253 concatenated marker set, subsampled
222 from the PhyloPhlAn dataset (Segata et al., 2013). Overall, the GTDB taxonomy was remarkably consistent
223 with comparable RED distributions for taxa at each investigated rank (**Fig. 2a,d; Fig. S13**). All GTDB taxa

224 were recovered as monophyletic or operationally monophyletic (**Fig S11**) for all supermatrix methods,
225 regardless of the underlying inference algorithm or model. The ASTRAL supertrees, inferred using the most
226 divergent approach tested, recovered 96% of GTDB taxa with ≥2 representatives as monophyletic or
227 operationally monophyletic (**Fig. S11**). The only major inconsistency affected the Euryarchaeota, with 48 taxa
228 being placed outside of this phylum in both supertrees (**Fig S14e, Fig S15**).
229
230 *Compositional bias and fast evolving sites*
231 To test for possible compositional bias we employed tools for character trimming and for clustering of high
232 confidence positional homology (*see Methods*) which have been shown to alleviate long branch attraction
233 artifacts and to increase tree accuracy for alignments of distantly-related sequences (Ali et al., 2019; Criscuolo
234 and Gribaldo, 2010). Decorated ML trees calculated from the trimmed or clustered alignments were in strong
235 taxonomic agreement with the reference tree, showing comparable RED values and recovering >96.5% of
236 GTDB taxa (with ≥2 representatives) as monophyletic or operationally monophyletic (**Fig. 2b ,c; Fig. S11;**
237 **Fig S13**). Less than 4% of genomes had conflicting taxonomic assignments at any rank above species (**Table**
238 **S11**), with the largest difference being observed in the class Methanosarcinia (18 taxa) and the order
239 Desulfurococcales (46 taxa) for the character trimmed alignment (**Fig S14d**). The clustered alignment
240 resulted in fewer differences, with a total of seven conflicting taxa (**Fig S14d**).
241
242 *Analysis of increasing genome database size*
243 An important variable in producing a genome-based taxonomy is the changing number of genome sequences
244 which will continue to increase in future and likely impact the underlying tree topology. To assess the
245 robustness of the GTDB taxonomy to this variable, we recapitulated the expansion of the archaeal genome
246 database since 2015 by subsampling the 1248 archaeal genomes according to their NCBI release date
247 resulting in 362, 528, 1035 and 1183 taxa for 2015 to 2018, respectively. Comparison of the taxonomy derived
248 from these antecedent trees to the reference tree revealed that >99% of all named taxa were recovered as
249 monophyletic groups suggesting that addition of new branches to the reference tree does not destabilise the
250 subset of robust interior nodes used for GTDB taxonomic assignments. This suggests that the GTDB
251 taxonomy should be stable with increasing dataset size.
252
253 *Rooting effects*
254 Rank normalization is sensitive to the placement of the tree root, which defines the last common ancestor
255 (set to RED=0) (Parks et al., 2020, 2018), and can therefore potentially influence the resulting taxonomy.
256 Since the rooting of both the archaeal and bacterial domains remains contested, GTDB uses an operational
257 approach whereby the median of multiple plausible rootings is considered (Parks et al., 2018). We assessed
258 the effect of fixed rooting of the archaeal domain on the taxonomy by testing two recently proposed archaeal
259 root placements; the first, within the Euryarchaeota (as currently defined by NCBI) (Raymann et al., 2015)
260 and the second, between the DPANN superphylum and all other Archaea (Williams et al., 2017). Overall,
261 RED values were stable across the tested rooting scenarios and the intervals defining taxonomic ranks in
262 GTDB were largely preserved (**Fig. 3**). As expected, a fixed root caused the taxa within the rooted lineages

263 to be drawn closer to the root, although it is important to note that absolute RED values should not be
264 compared between trees, or even between different rootings of the same tree. Rather the distribution of
265 labelled nodes within a rank is the key metric, and by this metric all taxa in the rooted lineages were within
266 their expected RED assigned rank intervals (**Fig S16; Fig. 3**).
267
268 **Proposal of new and revised taxa based on the GTDB taxonomy**.
269 After resolving polyphyletic groups and normalizing ranks, the archaeal GTDB taxonomy (release R04-RS89)
270 comprises 16 phyla, 36 classes, 96 orders, 238 families, 534 genera and 1248 species (**Table S12**). This
271 entailed the proposal of 13 new taxa and 32 new candidatus taxa above the rank of genus including five novel
272 species combinations and three novel candidatus species combinations (**Tables S13 to S16**). We also used
273 25 Latin names without standing in nomenclature as placeholders in the GTDB taxonomy (**Table S17)** to
274 preserve literature continuity. The extensive rearrangement of phyla to normalize phylogenetic depth resulted
275 in both division and amalgamation of release 89 NCBI phyla (**Fig. 4**). For example, the phylum Euryarchaeota
276 was divided into five separate phyla in the GTDB taxonomy due to its anomalous depth (**Fig. 1a; Fig 4**).
277 Names for three of the five phyla have previously been proposed; Methanobacteriota (Whitman et al., 2018),
278 Hadarchaeota (Chuvochina et al., 2019), and Hydrothermarchaeota (Chuvochina et al., 2019). Names for the
279 other two phyla are formally proposed in this study based on valid class names within each lineage;
280 Halobacteriota phyl. nov. (after the class Halobacteria) and Thermoplasmatota *phyl. nov.* (after the class
281 Thermoplasmata; **Table 1**, **Table S13**). Note that the name Euryarchaeota was not retained in the GTDB
282 taxonomy for two reasons: Firstly the name would be illegitimate if the rank of phylum is introduced into the
283 Code as a type was not designated in the original proposal (Woese et al., 1990), which is one of the
284 requirements for validation of a name. Secondly, the substantial changes made to this phylum may introduce
285 confusion if the name had been retained for one of the five newly circumscribed phyla. It is possible that the
286 name Euryarchaeota could be reintroduced as a superphylum, however, this is outside of the GTDB
287 taxonomy which only uses canonical ranks.
288
289 The TACK superphylum (Guy and Ettema, 2011) was reclassified as a single phylum based on rank
290 normalization and its robust monophyly, for which we propose to use the effectively published name
291 Thermoproteota (Whitman et al., 2018) based on the earliest validly described class for any TACK phylum,
292 the Thermoprotei (Reysenbach, 2001) (**Table 1**, **Table S13**). Note that alternatively the phylum name could
293 have been derived from the earliest genus name in the TACK superphylum, *Sulfolobus*, however this genus
294 is currently a member of the class Thermoprotei. The RED-based reorganisation of this lineage requires the
295 unification of the NCBI-defined TACK phyla as previously proposed (Petitjean et al., 2014). Thus the
296 Thaumarchaeota was reclassified as a class-level lineage, for which we propose an emended description of
297 the only validly described class in this lineage, the Nitrososphaeria (Stieglmeier et al., 2014) (**Fig. 5).**
298 According to its RED-based rank and concatenated protein phylogeny, the Aigarchaeota constitutes an order-
299 level lineage within the Nitrososphaeria, for which we propose the order Caldarchaeales *ord. nov.* (**Table**
300 **S15**) derived from the species *Ca.* Caldarchaeum subterraneum (Nunoura et al., 2011). We propose to
301 reclassify the NCBI-defined Crenarchaeota as an emended description of the class Thermoprotei and the

302 Korarchaeota as the Korarchaeia *class. nov.* (**Table S15**) based on the type species *Ca.* Korarchaeum
303 cryptofilum (Elkins et al., 2008). In addition, the candidate phyla Verstraetearchaeota (Vanwonterghem et al.,
304 2016) and Bathyarchaeota (Meng et al., 2014) were unified with the Thermoproteota based on their robust
305 phylogenetic affiliation. After unification, both lineages represent classes in the Thermoproteota for which the
306 names *Ca.* Methanomethylicia (Oren et al., 2020) from *Ca.* Methanomethylicus mesodigestum
307 (Vanwonterghem et al., 2016) and the GTDB placeholder name Bathyarchaeia (**Table S17**) were
308 implemented, until type material is assigned for the latter lineage (Chuvochina et al., 2019). Note that the
309 name Crenarchaeota was not retained in the GTDB taxonomy, *i.e.* used instead of the name Thermoproteota,
310 to avoid confusion over its recircumscription relative to the NCBI taxonomy, and because the name would be
311 illegitimate if the rank of phylum is introduced into the Code as per the Euryarchaeota (Woese et al., 1990).
312
313 Similar to the TACK superphylum, the recently described Asgard superphylum (Zaremba-Niedzwiedzka et
314 al., 2017) was reclassified as a single phylum for which we use Asgardarchaeota as a placeholder name
315 (**Table S17**) to retain its identity until type material has been proposed for this lineage (Chuvochina et al.,
316 2019), which potentially could be the recently described co-culture, *Ca.* Prometheoarchaeon syntrophicum
317 (Imachi et al., 2020). By contrast, the DPANN superphylum (Rinke et al., 2013) still comprises multiple (nine)
318 phyla after rank normalization in part due to a lack of stable deeper interior nodes for naming (**Fig. 4**). Many
319 of these phyla are represented by only a few genomes on long branches often reflected by low bootstrap
320 support (**Fig. S17**). We envision that the DPANN phyla will undergo further reclassification in future GTDB
321 releases when additional genomes become available to populate this region of the tree, however, even if
322 some these phyla were unified, DPANN cannot be collapsed into a single phylum according to rank
323 normalization.
324
325 Unlike the major changes required at the phylum level, archaeal taxa with lower rank information (species to
326 class) were more stable, with an average of only 11% name changes. Notable examples include the well-
327 known genus *Sulfolobus*, which was reported early on as potentially polyphyletic (Fuchs et al., 1996) and is
328 comprised of strains differing in their metabolic repertoire and genome size (Quehenberger et al., 2017). The
329 concatenated protein tree confirms that *Sulfolobus* is not monophyletic, being interspersed with species
330 belonging to the genera *Acidanus, Metallosphaera* and *Sulfurisphaera.* We resolved this polyphyly by dividing
331 the group into four separate genera (**Fig. S18**) reflecting previously reported differences between *Sulfolobus*
332 species, including a high number of transposable elements in *Sulfolobus_A* species (*S. islandicus* and *S.*
333 *solfataricus*), which are mostly absent in the type species of the genus, *Sulfolobus acidocaldarius*
334 (Quehenberger et al., 2017). An example of a more complicated situation is the taxonomy of genera belonging
335 to the halophilic family Natrialbaceae. Some of these genera have been reported as polyphyletic such as
336 *Natrinema* and *Haloterrigena* (Minegishi et al., 2010), or are polyphyletic in published trees without associated
337 comment, including *Halopiger* (Sorokin et al., 2019) and *Natronolimnobius* (Sorokin et al., 2018). We
338 confirmed this polyphyly in the concatenated protein tree, which required extensive reclassification guided by
339 the type species of each genus (**Fig S19, Table S14)**.
340

341 # Discussion

342 Here we present the Genome Taxonomy Database (GTDB) for the domain Archaea to provide a
343 phylogenetically congruent and rank-normalized classification based on well-supported nodes in a
344 phylogenomic tree of 122 concatenated conserved single copy marker proteins (**Table S2**). Unlike the
345 bacterial GTDB reference tree comprising ~19 fold more species representatives (Parks et al., 2020), the
346 relatively modest number of publicly available archaeal genomes representing only 1248 species allowed us
347 to use IQ-TREE with a protein mixture model that captures substitution site heterogeneity between sites and
348 can mitigate long branch attraction artifacts (Wang et al., 2018). The proposed taxonomy is stable under a
349 range of standard phylogenetic variables, including alternate marker genes, inference methods, tree rooting
350 scenarios and expansion of the genome database, due in part to the inherent flexibility of rank designations
351 within RED intervals (**Fig. 1**). We endeavoured to preserve the existing archaeal taxonomy wherever possible,
352 however the great majority (93.3%) of the 2239 archaeal genomes in GTDB had one or more changes to
353 their classification compared to the NCBI taxonomy (**Fig. 1c**). This high percentage of modifications,
354 compared to 58% reported for genomes in the bacterial GTDB (Parks et al., 2018), could be attributed to
355 extreme unevenness observed within archaeal ranks, particularly at the phylum level. For example, the
356 division of the NCBI-defined Euryarchaeota alone affected over two thirds of all archaeal genomes (**Fig. 4**).
357 Secondly, widespread missing rank information in NCBI r89, particularly amongst as-yet-uncultivated
358 lineages, required numerous passive (rank filling) changes to the taxonomy (**Fig. 1**). And thirdly, the Bacteria
359 have highly sampled species and genera that did not require taxonomic changes, including over 12,000
360 *Streptococcus* genomes in release 04-RS89, which effectively lowers the percentage of bacterial genomes
361 with taxonomic differences to NCBI.
362
363 The 7-fold difference in the number of archaeal and bacterial phyla (16 vs 112; release 04-RS89) is notable
364 and raises the question of whether GTDB-defined bacterial and archaeal phyla are comparable. Strictly
365 speaking they are not, as each taxonomy was developed independently and shaped around the existing NCBI
366 taxonomy as far as possible. Early attempts to produce a prokaryotic concatenated protein tree upon which
367 to base a combined taxonomy distorted RED values to the point of being unusable (data not shown). In the
368 case of the Archaea, we also experimented with moving the phylum and class rank intervals to the right (away
369 from the root) since the starting distributions were so broad (Fig. 1a), which more than doubled the number
370 of archaeal phyla. However, this also resulted in an even greater departure from the starting NCBI taxonomy
371 and hence was not pursued further. Perhaps the most compelling evidence that the current ratio of phyla may
372 reflect true biological diversity is the fact that there are ~19-fold more ANI-defined bacterial than archaeal
373 species (1248 vs 23,458; release 04-RS89).

374 The archaeal GTDB taxonomy and associated tree and alignment files are available online
375 (https://gtdb.ecogenomic.org) and via linked third party tools, e.g. AnnoTree (Mendler et al., 2019). Users can
376 classify their own genomes against the archaeal GTDB taxonomy using GTDB-Tk (Chaumeil et al., 2019).

377 We envisage that in the short term, the archaeal taxonomy will scale with genome deposition in the public
378 repositories based on current accumulation rates (**Fig. S20**). However, in the longer term more efficient
379 phylogenomic tools will be needed to scale with increasingly large genomic datasets and to allow for
380 biologically meaningful phylogenetic inferences. We also expect that less stable parts of the concatenated
381 protein tree, *e.g.* the DPANN phyla, will become more robust with additional genome sequence
382 representatives.

383

384 # Methods

385 **Genome dataset**

386 For the archaeal GTDB taxonomy R04-RS89 we obtained 2,661 archaeal genomes from RefSeq/GenBank
387 release 89 and augmented them with 187 phylogenetically diverse MAGs derived from the Sequencing Read
388 Archive (SRA, (Haft et al., 2018)) as part of a large genome recovery study (Parks et al., 2017), resulting in
389 2,848 genomes. This data set was refined by applying a quality threshold (completeness - 5x contamination
390 >50%) using lineage specific markers implemented in CheckM (Parks et al., 2019, 2015), and by screening
391 out genomes which contain <40% of the 122 archaeal GTDB marker genes, more than 100,000 ambiguous
392 bases, more than 1000 contigs, and which have an N50 <5kb. The filtered genomes were manually inspected
393 and four exceptions were made for genomes of high nomenclatural or taxonomic significance (**Table S22).**
394 This approach left 2,392 genomes to form species clusters (see below), resulting in a total 1248 species
395 representative genomes for the downstream analysis (**Table S1**). The 456 genomes which did not pass QC
396 are still searchable on the GTDB website (https://gtdb.ecogenomic.org/) and are listed in **table S20**.

397

398 **NCBI taxonomy**

399 The NCBI taxonomy of all representative genomes of R04-RS89 was obtained from the NCBI Taxonomy FTP
400 site on July 16th, 2018. The NCBI taxonomy was standardized to seven ranks (species to domain) by
401 identifying missing standard ranks and filling these gaps with rank prefixes and by removing non-standard
402 ranks (Parks et al., 2018). All standard ranks were prefixed with rank identifiers (e.g. "p__" for phylum) as
403 previously described (McDonald et al., 2012).

404

405 **Phylogenomic marker set**

406 Archaeal multiple sequence alignments (MSAs) were created through the concatenation of 122
407 phylogenetically informative markers comprised of proteins or protein domains specified in the Pfam v27 or
408 TIGRFAMs v15.0 databases. The 122 archaeal marker proteins were selected based on the criteria described
409 in (Parks et al., 2017). In brief, this included being present in ≥90% of archaeal genomes, and, when present,
410 single-copy in ≥95% of genomes. Only genomes comprising ≤200 contigs with an N50 of ≥20 kb and with
411 CheckM completeness and contamination estimates of ≥95% and ≤5%, respectively, were considered.

412 Phylogenetically informative proteins were determined by filtering ubiquitous proteins whose gene trees had
413 poor congruence with a set of subsampled concatenated genome trees (Parks et al., 2017). Gene calling was
414 performed with Prodigal v2.6.3, and markers were identified and aligned using HMMER v3.1b1. The presence
415 and absence of the 122 protein markers in the 1248 species representatives is provided in **table S21**. The
416 marker proteins were concatenated into a multiple sequence alignment (MSA) of 32.5k columns, to which we
417 refer as "untrimmed MSA" in this manuscript. To remove sites with weak phylogenetic signals, we created an
418 amino acid alignment by trimming columns represented in <50% of the genomes and columns with less than
419 25% or more than 95% amino acid consensus, resulting in an initial 27,000 amino acid alignment (Suppl text).
420 Thereby, the term consensus refers to the number of taxa with the same residue in a given sequence
421 alignment column, e.g. a maximum consensus of 95% means that a maximum of 95% of all taxa can have
422 the same residue in an alignment column in order to be considered for the trimmed alignment. To reduce
423 computational requirements, the alignment was further trimmed by randomly selecting 42 amino acids from
424 the remaining columns of each marker. The resulting ar122.r89 MSA included a total of 5124 (42*122)
425 columns. This MSA filtering methodology is implemented in the `align` method of GTDB-Tk v1.0.2 (Chaumeil
426 et al., 2019).
427
428 **Alternative supermatrix marker sets**
429 Alternative MSAs, resembling previously published datasets, were created through the concatenation of 16
430 ribosomal proteins, termed dataset rp1 (Hug et al., 2016) and 23 ribosomal proteins, termed rp2 (Rinke et
431 al., 2013). After trimming columns represented by <50% of the genomes and with an amino acid consensus
432 <25%, the resulting MSA spanned 1174 and 2377 amino acids for rp1 and rp2, respectively.
433 In addition we created a MSA from 53 recently proposed archaeal marker proteins (ar.53; Table S8)
434 (Dombrowski et al., 2020), by creating individual alignments for each of the 53 HMMs for all 1248 species
435 representatives, using pfam 33.1 and tigrfam 15.0. The resulting concatenated MSA of 13,451 amino acids
436 was used without further trimming steps to infer phylogenetic trees or to apply tools addressing compositional
437 bias.
438
439 **SSU rRNA gene**
440 Archaeal SSU rRNA genes were identified from the 1248 archaeal R04-RS89 GTDB genomes using nhmmer
441 v3.1b2 (Wheeler and Eddy, 2013) with the SSU rRNA model (RF00177) from the RFAM database (Kalvari et
442 al., 2018). Only the longest sequence was retained per genome. The resulting sequences were aligned with
443 SSU-ALIGN 0.1.1 (Nawrocki, 2009), regions of low posterior probabilities, which are indicative of high
444 alignment ambiguity were pruned with ssu-mask (SSU-ALIGN 0.1.1). The alignment was trimmed with an in-
445 house script (trimSeqs.py v0.0.1; module bioscripts) to remove poorly represented leading and trailing
446 positions, along with short sequences below 900bp
447 (https://github.com/Ecogenomics/scripts/blob/master/scripts/trimSeqs.py).
448
449 **Species cluster**

450 The 2,392 archaeal genomes were formed into species clusters as previously described (Parks et al., 2020).
451 Briefly, a representative genome was selected for each of the 380 validly or effectively published archaeal
452 species with one or more genomes passing quality control and genomes assigned to these representatives
453 using average nucleotide identity (ANI) and alignment fraction (AF) criteria. Thereby, genomes were assigned
454 to the closest representative genome for which they have an ANI of 95% ANI, with an AF of at least 65%,
455 except if two representatives had an ANI >95%. In such cases, the ANI radius of a representative was set to
456 the value of the closest representative up to a maximum of 97%, with species representatives having an ANI
457 >97% considered synonyms. Genomes not assigned to one of these 380 species were formed into 868 *de*
458 *novo* species clusters, each specified by a single representative genome. Representative genomes were
459 selected based on assembly quality with preference given to isolate genomes. Of the 868 de novo species
460 clusters, the representative genomes of 70 were unnamed isolates, 775 were MAGs and 23 were SAGs.
461

462 **Accounting for compositional bias**

463 Each of the untrimmed 122 GTDB r89 archaeal single-copy marker protein alignments was filtered individually
464 using BMGE 1.12 (Criscuolo and Gribaldo, 2010) and Divvier 1.0 (Ali et al., 2019). BMGE was executed using
465 -t AA -s FAST -h 0.55 -m BLOSUM30, and Divvier was run using the recommended options: -divvy -mincol 4
466 -divvygap. Processing untrimmed protein alignments of individual markers ensures that all protein positions
467 are considered when accounting for compositional bias. Next, each of the filtered marker gene alignments
468 were concatenated into a single MSA supermatrix for BMGE and one for Divvier, respectively, whereby
469 previously removed gap-only sequences were added again in the corresponding positions. Finally, the MSA
470 was trimmed according to GTDB criteria mentioned above to a length of 7859 amino acids (BMGE) and
471 32061 amino acids (Divvier) and used for phylogenetic inferences (see below).
472

473 **Phylogenetic inference**

474 Phylogenomic trees were inferred with FastTree 2 (Price et al., 2010), ExaML (Kozlov et al., 2015), IQ-TREE
475 (Nguyen et al., 2015), and PhyloBayes (Lartillot and Philippe, 2004) on different alignments and with a range
476 of models (**Table S10**). Note that we chose IQ-TREE as the GTDB standard inference, since it scales with
477 our dataset, allows mixture models (see below), and because a previous study concluded that for
478 concatenation-based species tree inference, IQ-TREE consistently achieved the best-observed likelihoods
479 for all data sets, compared to RAxML/ExaML and FastTree (Zhou et al., 2018). More details about each
480 inference program is provided below.
481

482 ***FastTree***

483 FastTree v2.1.9 was executed in multithreaded mode with the WAG+GAMMA parameters.
484

485 ***IQ-TREE***

486 IQ-TREE was executed employing mixture models, such as C10-C60 (Le et al. 2008), and a faster
487 approximation of these models known as "posterior mean site frequency" (PMSF) model (Wang et al., 2018).
488 True C10-C60 trees are computationally more demanding, whereby memory requirements tend to increase

489 with the number of components in the mixture, ranging from 10 to 60 (**Table S10**), and we therefore opted
490 for the faster PMSF model, in particular C10 PMSF, to calculate the ar122.r89 tree. The tree was calculated
491 with IQ-TREE v1.6.12 based on the C10 mixture model and a starting tree (-ft), inferred by FastTree v2.1.9
492 as described above, to invoke the faster PMSF approximation with the following settings: *-m LG+C10+F+G*
493 *-ft <starting tree>*.
494
495 ***ExaML***
496 ExaML trees (gamma, JTT) were calculated from 10 different starting trees with random seeds using the mpi
497 version 3.0.20 (settings: -m GAMMA), whereby the tree with the highest likelihood score was retained.
498
499 ***PhyloBayes***
500 To accommodate the computationally demanding Bayesian inferences we subsampled our data set by
501 reducing the number of taxa to one representative per order resulting in 96 taxa. The order representatives
502 were selected by removing genomes with a quality score (CheckM completeness - 5*CheckM contamination)
503 of <50; <50% of the 122 archaeal marker genes; an N50 <4 Kb; >2,500 contigs or >1,500 scaffolds). From
504 the remaining genomes, the highest quality genome was selected giving preference to i) NCBI reference
505 genome annotated as "complete" at NCBI, ii) NCBI reference genomes, iii) complete NCBI representative
506 genomes, iv) NCBI representative genomes, and v) GTDB representative genomes. **Table S19** indicates
507 which of these categories a genome falls into. The Bayesian trees were inferred with PhyloBayes-MPI version
508 1.10.2 with the following settings*: -cat -gtr -x 10 -1 -dgam 4*. Three independent chains were run and tested
509 for convergence (maxdiff =0.13) using bpcomp (part of pb_mpi) whereby the first 1,000 trees were eliminated
510 as burn-in and the remaining trees were sampled every 10 trees.
511
512 ***Supertree***
513 Supertrees were calculated from 1) 122 GTDB markers, and 2) from 253 markers which were present in
514 >10% of archaeal genomes and were extracted from the PhyloPhlAn dataset (Segata et al., 2013).
515 For the 122 marker set, a guide tree was inferred for each marker gene via approximate ML using FastTree
516 v2.1.9 with the WAG model and gamma distributed rate heterogeneity. Subsequently, a complete ML tree
517 was inferred using IQ-Tree v 1.6.9 with the C10 + PMSF model and the guide tree with 100 non-parametric
518 bootstrap samplings to assess node support. A consensus tree was constructed from the individual gene
519 trees using ASTRAL v5.6.3.
520 For the 253 marker set, we first identified, 400 conserved, single-copy gene orthologues from the PhyloPhlAn
521 data set (Segata et al., 2013) using PhyloPhlAn v0.99. Markers present in less than 10% of all archaeal
522 genomes were identified and removed resulting in a final marker set of 253 protein markers. For each marker,
523 multiple-sequence alignment was performed using MAFFT-LINSI v7.221 (Katoh and Standley, 2013) and the
524 resulting amino acid alignment was filtered using trimAl 1.2rev59, removing columns present in less than half
525 of all taxa in the alignment. Tree inference was performed using the same approach as for the 122 marker
526 set.
527

528 ***SSU trees***

529 Trees from the trimmed SSU gene alignments (see section "SSU rRNA gene" above) were inferred with IQ-
530 TREE, whereby the substitution model was determined by IQ-TREEs model finder to be SYM+R10.

531

532 **Taxonomic assignment and rank standardisation**

533 The assignment of higher taxonomic ranks was normalized based on the relative evolutionary distance (RED)
534 calculated from the ar122.r89 tree using PhyloRank (v0.0.37; https://github.com/dparks1134/PhyloRank/) as
535 described previously (Parks et al., 2018). In brief, PhyloRank linearly interpolates the RED values of internal
536 nodes according to lineage-specific rates of evolution under the constraints of the root being defined as zero
537 and the RED of all present taxa being defined as one. To account for the influence of the root placement on
538 RED values PhyloRank roots a tree multiple times, at the midpoint of each phylum with two or more classes.
539 In the case of the ar122.r89 reference tree, PhyloRank identified 5 GTDB phyla (Halobacteriota,
540 Thermoplasmatota, Methanobacteriota, Thermoproteota, and Asgardarchaeota) with two or more classes to
541 be used for the multiple outgroup rooting approach. The RED of a taxon is then calculated as the median
542 RED over all these tree rootings, excluding the tree in which the taxon was the outgroup. The RED intervals
543 for each rank were defined as the median RED value ±0.1 to serve as a guide for the normalization of
544 taxonomic ranks from genus to phylum in GTDB. The rank of species was assigned using ANI and AF criteria
545 (see above). Note, that the application of names above the rank of genus in the GTDB taxonomy is manually
546 curated where required, i.e. where naming ambiguity exists due to reclassification changes (taxa split, union,
547 transfer) or where a new name needs to be assigned. Thereby, the curation team follows a decision tree for
548 the manual curation workflow (**Fig. S21, Suppl. Text**).

549

550 **Assessment of phylogenetic congruence**

551 We measured the phylogenetic tree similarity applying the normalized Robinson-Foulds distance (RF) of each
552 alternative tree compared to the ar122.89 tree. The RF distance is defined as the number of splits that are
553 present in one tree but not in the other one, and vice versa (Robinson and Foulds, 1981). The normalized RF
554 is a relative measure obtained by dividing the calculated Robison-Foulds distance by the maximal RF. The
555 resulting distance is a value between 0% and 100%, which can be interpreted as the percentage of different
556 or missing splits in the alternative trees compared to the ar.122.89 tree (Kupczok et al., 2010). RF calculations
557 and tree comparisons with lineage resolution were carried out with the visualisation tool metatree
558 (https://github.com/aaronmussig/metatree).

559

560 **Assessment of taxonomic congruence**

561 The congruence of the GTDB taxonomy in different trees was assessed as (i) the percentage of taxa identified
562 as monophyletic, operationally monophyletic, defined as having an F measure $\geq$0.95, or polyphyletic, (ii) the
563 RED distributions for taxa at each rank relative to the median RED value of that rank, and (iii) the number of
564 genomes with identical or conflicting taxonomic assignments between compared trees. Thereby (i) was
565 carried out by placing each taxon on the node with the highest resulting F measure, which is defined as the
566 harmonic mean of precision and recall, and it has been proposed for decorating trees with a donor taxonomy

(McDonald et al., 2012). Note, we introduced the term operationally monophyletic (F measure ≥0.95), since otherwise a few incongruent genomes can cause a large number of polyphyletic taxa.

Data availability

The GTDB taxonomy is available at the GTDB website (https://gtdb.ecogenomic.org/), including the ar122.r89 tree and the GTDB and NCBI taxonomic assignments for all 2,392 archaeal genomes in GTDB 04-RS89. The standalone tool GTDB-Tk, which enables researchers to classify their own genomes according to the GTDB taxonomy is available at GitHub (https://github.com/Ecogenomics/GTDBTk/) and through KBase (https://kbase.us/applist/apps/ kb_gtdbtk/run_kb_gtdbtk/release). Genome assemblies are available from the NCBI Assembly database (BioProject: PRJNA593905).

Acknowledgements

We thank Brian Kemish and Dinindu Senanayake for system administration support, Pelin Yilmaz for stimulating discussions on archaeal taxonomy, and the GTDB user community for their feedback. We also thank the Australian Centre for Ecogenomics (ACE) at The University of Queensland and the New Zealand eScience Infrastructure (NeSI) for providing high performance computing facilities. The project was supported by an Australian Research Council (ARC) Future Fellowship (FT170100213) awarded to C.R. and by an Australian Research Council Laureate Fellowship (FL150100038) awarded to P.H.

References

Adam, P.S., Borrel, G., Brochier-Armanet, C., Gribaldo, S., 2017. The growing tree of Archaea: new perspectives on their diversity, evolution and ecology. ISME J. https://doi.org/10.1038/ismej.2017.122

Ali, R.H., Bogusz, M., Whelan, S., 2019. Identifying Clusters of High Confidence Homologies in Multiple Sequence Alignments. Mol. Biol. Evol. 36, 2340–2351. https://doi.org/10.1093/molbev/msz142

Baker, B.J., Comolli, L.R., Dick, G.J., Hauser, L.J., Hyatt, D., Dill, B.D., Land, M.L., VerBerkmoes, N.C., Hettich, R.L., Banfield, J.F., 2010. Enigmatic, ultrasmall, uncultivated Archaea. PNAS 107, 8806–8811. https://doi.org/10.1073/pnas.0914470107

Baker, B.J., De Anda, V., Seitz, K.W., Dombrowski, N., Santoro, A.E., Lloyd, K.G., 2020. Diversity, ecology and evolution of Archaea. Nature Microbiology 5, 887–900. https://doi.org/10.1038/s41564-020-0715-z

Barns, S.M., Delwiche, C.F., Palmer, J.D., Pace, N.R., 1996. Perspectives on archaeal diversity, thermophily and monophyly from environmental rRNA sequences. Proc Natl Acad Sci U S A 93, 9188–9193.

601 Brochier-Armanet, C., Boussau, B., Gribaldo, S., Forterre, P., 2008. Mesophilic crenarchaeota: proposal for
602 a third archaeal phylum, the Thaumarchaeota. Nat Rev Micro 6, 245–252.
603 https://doi.org/10.1038/nrmicro1852
604 Castelle, C.J., Wrighton, K.C., Thomas, B.C., Hug, L.A., Brown, C.T., Wilkins, M.J., Frischkorn, K.R.,
605 Tringe, S.G., Singh, A., Markillie, L.M., Taylor, R.C., Williams, K.H., Banfield, J.F., 2015. Genomic
606 Expansion of Domain Archaea Highlights Roles for Organisms from New Phyla in Anaerobic Carbon
607 Cycling. Current Biology 16, 690–701. https://doi.org/10.1016/j.cub.2015.01.014
608 Chaumeil, P.-A., Mussig, A.J., Hugenholtz, P., Parks, D.H., 2019. GTDB-Tk: a toolkit to classify genomes
609 with the Genome Taxonomy Database. Bioinformatics. https://doi.org/10.1093/bioinformatics/btz848
610 Chuvochina, M., Rinke, C., Parks, D.H., Rappé, M.S., Tyson, G.W., Yilmaz, P., Whitman, W.B.,
611 Hugenholtz, P., 2019. The importance of designating type material for uncultured taxa. Systematic
612 and Applied Microbiology, Taxonomy of uncultivated Bacteria and Archaea 42, 15–21.
613 https://doi.org/10.1016/j.syapm.2018.07.003
614 Criscuolo, A., Gribaldo, S., 2010. BMGE (Block Mapping and Gathering with Entropy): a new software for
615 selection of phylogenetic informative regions from multiple sequence alignments. BMC Evolutionary
616 Biology 10, 210. https://doi.org/10.1186/1471-2148-10-210
617 Dombrowski, N., Williams, T.A., Sun, J., Woodcroft, B.J., Lee, J.-H., Minh, B.Q., Rinke, C., Spang, A., 2020.
618 Undinarchaeota illuminate DPANN phylogeny and the impact of gene transfer on archaeal evolution.
619 Nature Communications 11, 3939. https://doi.org/10.1038/s41467-020-17408-w
620 Elkins, J.G., Podar, M., Graham, D.E., Makarova, K.S., Wolf, Y., Randau, L., Hedlund, B.P., Brochier-
621 Armanet, C., Kunin, V., Anderson, I., Lapidus, A., Goltsman, E., Barry, K., Koonin, E.V., Hugenholtz,
622 P., Kyrpides, N., Wanner, G., Richardson, P., Keller, M., Stetter, K.O., 2008. A korarchaeal genome
623 reveals insights into the evolution of the Archaea. Proceedings of the National Academy of Sciences
624 105, 8102–8107. https://doi.org/10.1073/pnas.0801980105
625 Federhen, S., 2012. The NCBI Taxonomy database. Nucleic Acids Res 40, D136–D143.
626 https://doi.org/10.1093/nar/gkr1178
627 Fuchs, T., Huber, H., Burggraf, S., Stetter, K.O., 1996. 16S rDNA-based Phylogeny of the Archaeal Order
628 Sulfolobales and Reclassification of Desulfurolobus ambivalens as Acidianus ambivalens comb.
629 nov. Systematic and Applied Microbiology 19, 56–60. https://doi.org/10.1016/S0723-2020(96)80009-
630 9
631 Gribaldo, S., Brochier-Armanet, C., 2006. The origin and evolution of Archaea: a state of the art. Philos
632 Trans R Soc Lond B Biol Sci 361, 1007–1022. https://doi.org/10.1098/rstb.2006.1841
633 Guy, L., Ettema, T.J.G., 2011. The archaeal 'TACK' superphylum and the origin of eukaryotes. Trends in
634 Microbiology 19, 580–587. https://doi.org/10.1016/j.tim.2011.09.002
635 Guy, L., Spang, A., Saw, J.H., Ettema, T.J.G., 2014. 'Geoarchaeote NAG1' is a deeply rooting lineage of
636 the archaeal order Thermoproteales rather than a new phylum. ISME J 8, 1353–1357.
637 https://doi.org/10.1038/ismej.2014.6
638 Haft, D.H., DiCuccio, M., Badretdin, A., Brover, V., Chetvernin, V., O'Neill, K., Li, W., Chitsaz, F.,
639 Derbyshire, M.K., Gonzales, N.R., Gwadz, M., Lu, F., Marchler, G.H., Song, J.S., Thanki, N.,
640 Yamashita, R.A., Zheng, C., Thibaud-Nissen, F., Geer, L.Y., Marchler-Bauer, A., Pruitt, K.D., 2018.
641 RefSeq: an update on prokaryotic genome annotation and curation. Nucleic Acids Res 46, D851–
642 D860. https://doi.org/10.1093/nar/gkx1068
643 Hallam, S.J., Konstantinidis, K.T., Putnam, N., Schleper, C., Watanabe, Y., Sugahara, J., Preston, C., de la
644 Torre, J., Richardson, P.M., DeLong, E.F., 2006. Genomic analysis of the uncultivated marine
645 crenarchaeote Cenarchaeum symbiosum. Proc. Natl. Acad. Sci. U.S.A. 103, 18296–18301.
646 https://doi.org/10.1073/pnas.0608549103
647 Huber, H., Hohn, M.J., Rachel, R., Fuchs, T., Wimmer, V.C., Stetter, K.O., 2002. A new phylum of Archaea
648 represented by a nanosized hyperthermophilic symbiont. Nature 417, 63–67.
649 https://doi.org/10.1038/417063a
650 Hug, L.A., Baker, B.J., Anantharaman, K., Brown, C.T., Probst, A.J., Castelle, C.J., Butterfield, C.N.,
651 Hernsdorf, A.W., Amano, Y., Ise, K., Suzuki, Y., Dudek, N., Relman, D.A., Finstad, K.M., Amundson,
652 R., Thomas, B.C., Banfield, J.F., 2016. A new view of the tree of life. Nature Microbiology 1, 16048.
653 https://doi.org/10.1038/nmicrobiol.2016.48
654 Kalvari, I., Argasinska, J., Quinones-Olvera, N., Nawrocki, E.P., Rivas, E., Eddy, S.R., Bateman, A., Finn,
655 R.D., Petrov, A.I., 2018. Rfam 13.0: shifting to a genome-centric resource for non-coding RNA
656 families. Nucleic Acids Res. 46, D335–D342. https://doi.org/10.1093/nar/gkx1038
657 Katoh, K., Standley, D.M., 2013. MAFFT Multiple Sequence Alignment Software Version 7: Improvements
658 in Performance and Usability. Mol Biol Evol 30, 772–780. https://doi.org/10.1093/molbev/mst010

Kozlov, A.M., Aberer, A.J., Stamatakis, A., 2015. ExaML version 3: a tool for phylogenomic analyses on supercomputers. Bioinformatics 31, 2577–2579. https://doi.org/10.1093/bioinformatics/btv184

Kozubal, M.A., Romine, M., Jennings, R. deM, Jay, Z.J., Tringe, S.G., Rusch, D.B., Beam, J.P., McCue, L.A., Inskeep, W.P., 2013. Geoarchaeota: a new candidate phylum in the Archaea from high-temperature acidic iron mats in Yellowstone National Park. ISME J 7, 622–634. https://doi.org/10.1038/ismej.2012.132

Kupczok, A., Schmidt, H.A., von Haeseler, A., 2010. Accuracy of phylogeny reconstruction methods combining overlapping gene data sets. Algorithms Mol Biol 5, 37. https://doi.org/10.1186/1748-7188-5-37

Lartillot, N., Philippe, H., 2004. A Bayesian Mixture Model for Across-Site Heterogeneities in the Amino-Acid Replacement Process. Mol Biol Evol 21, 1095–1109. https://doi.org/10.1093/molbev/msh112

Marin, J., Battistuzzi, F.U., Brown, A.C., Hedges, S.B., 2017. The Timetree of Prokaryotes: New Insights into Their Evolution and Speciation. Molecular Biology and Evolution 34, 437–446. https://doi.org/10.1093/molbev/msw245

McDonald, D., Price, M.N., Goodrich, J., Nawrocki, E.P., DeSantis, T.Z., Probst, A., Andersen, G.L., Knight, R., Hugenholtz, P., 2012. An improved Greengenes taxonomy with explicit ranks for ecological and evolutionary analyses of bacteria and archaea. ISME J 6, 610–618. https://doi.org/10.1038/ismej.2011.139

Mendler, K., Chen, H., Parks, D.H., Lobb, B., Hug, L.A., Doxey, A.C., 2019. AnnoTree: visualization and exploration of a functionally annotated microbial tree of life. Nucleic Acids Res. https://doi.org/10.1093/nar/gkz246

Meng, J., Xu, J., Qin, D., He, Y., Xiao, X., Wang, F., 2014. Genetic and functional properties of uncultivated MCG archaea assessed by metagenome and gene expression analyses. ISME J 8, 650–659. https://doi.org/10.1038/ismej.2013.174

Minegishi, H., Kamekura, M., Itoh, T., Echigo, A., Usami, R., Hashimoto, T., 2010. Further refinement of the phylogeny of the Halobacteriaceae based on the full-length RNA polymerase subunit B′ (rpoB′) gene. International Journal of Systematic and Evolutionary Microbiology 60, 2398–2408. https://doi.org/10.1099/ijs.0.017160-0

Murray, R.G.E., Stackebrandt, E., 1995. Taxonomic Note: Implementation of the Provisional Status Candidatus for Incompletely Described Procaryotes. International Journal of Systematic and Evolutionary Microbiology 45, 186–187. https://doi.org/10.1099/00207713-45-1-186

Nawrocki, E., 2009. Structural RNA Homology Search and Alignment Using Covariance Models. All Theses and Dissertations (ETDs). https://doi.org/10.7936/K78050MP

Nguyen, L.-T., Schmidt, H.A., von Haeseler, A., Minh, B.Q., 2015. IQ-TREE: A Fast and Effective Stochastic Algorithm for Estimating Maximum-Likelihood Phylogenies. Mol Biol Evol 32, 268–274. https://doi.org/10.1093/molbev/msu300

Nunoura, T., Takaki, Y., Kakuta, J., Nishi, S., Sugahara, J., Kazama, H., Chee, G.-J., Hattori, M., Kanai, A., Atomi, H., Takai, K., Takami, H., 2011. Insights into the evolution of Archaea and eukaryotic protein modifier systems revealed by the genome of a novel archaeal group. Nucleic Acids Res 39, 3204–3223. https://doi.org/10.1093/nar/gkq1228

Oren, A., 2017. A plea for linguistic accuracy – also for Candidatus taxa. International Journal of Systematic and Evolutionary Microbiology 67, 1085–1094. https://doi.org/10.1099/ijsem.0.001715

Oren, A., da Costa, M.S., Garrity, G.M., Rainey, F.A., Rosselló-Móra, R., Schink, B., Sutcliffe, I., Trujillo, M.E., Whitman, W.B., 2015. Proposal to include the rank of phylum in the International Code of Nomenclature of Prokaryotes. International Journal of Systematic and Evolutionary Microbiology 65, 4284–4287. https://doi.org/10.1099/ijsem.0.000664

Oren, A., Garrity, G.M., Parker, C.T., Chuvochina, M., Trujillo, M.E., 2020. Lists of names of prokaryotic Candidatus taxa. International Journal of Systematic and Evolutionary Microbiology. https://doi.org/10.1099/ijsem.0.003789

Parker, C.T., Tindall, B.J., Garrity, G.M., 2019. International Code of Nomenclature of Prokaryotes. International Journal of Systematic and Evolutionary Microbiology, 69, S1–S111. https://doi.org/10.1099/ijsem.0.000778

Parks, D.H., Chuvochina, M., Chaumeil, P.-A., Rinke, C., Mussig, A.J., Hugenholtz, P., 2020. A complete domain-to-species taxonomy for Bacteria and Archaea. Nature Biotechnology 1–8. https://doi.org/10.1038/s41587-020-0501-8

Parks, D.H., Chuvochina, M., Chaumeil, P.-A., Rinke, C., Mussig, A.J., Hugenholtz, P., 2019. Selection of representative genomes for 24,706 bacterial and archaeal species clusters provide a complete genome-based taxonomy. bioRxiv 771964. https://doi.org/10.1101/771964

Parks, D.H., Chuvochina, M., Waite, D.W., Rinke, C., Skarshewski, A., Chaumeil, P.-A., Hugenholtz, P., 2018. A standardized bacterial taxonomy based on genome phylogeny substantially revises the tree of life. Nature Biotechnology 36, 996–1004. https://doi.org/10.1038/nbt.4229

Parks, D.H., Imelfort, M., Skennerton, C.T., Hugenholtz, P., Tyson, G.W., 2015. CheckM: assessing the quality of microbial genomes recovered from isolates, single cells, and metagenomes. Genome Res. 25, 1043–1055. https://doi.org/10.1101/gr.186072.114

Parks, D.H., Rinke, C., Chuvochina, M., Chaumeil, P.-A., Woodcroft, B.J., Evans, P.N., Hugenholtz, P., Tyson, G.W., 2017. Recovery of nearly 8,000 metagenome-assembled genomes substantially expands the tree of life. Nature Microbiology 2, 1533–1542. https://doi.org/10.1038/s41564-017-0012-7

Petitjean, C., Deschamps, P., López-García, P., Moreira, D., 2014. Rooting the Domain Archaea by Phylogenomic Analysis Supports the Foundation of the New Kingdom Proteoarchaeota. Genome Biol Evol 7, 191–204. https://doi.org/10.1093/gbe/evu274

Petitjean, C., Deschamps, P., López-García, P., Moreira, D., Brochier-Armanet, C., 2015. Extending the conserved phylogenetic core of archaea disentangles the evolution of the third domain of life. Mol. Biol. Evol. 32, 1242–1254. https://doi.org/10.1093/molbev/msv015

Price, M.N., Dehal, P.S., Arkin, A.P., 2010. FastTree 2 – Approximately Maximum-Likelihood Trees for Large Alignments. PLoS ONE 5, e9490. https://doi.org/10.1371/journal.pone.0009490

Probst, A.J., Ladd, B., Jarett, J.K., Geller-McGrath, D.E., Sieber, C.M.K., Emerson, J.B., Anantharaman, K., Thomas, B.C., Malmstrom, R.R., Stieglmeier, M., Klingl, A., Woyke, T., Ryan, M.C., Banfield, J.F., 2018. Differential depth distribution of microbial function and putative symbionts through sediment-hosted aquifers in the deep terrestrial subsurface. Nature Microbiology 3, 328. https://doi.org/10.1038/s41564-017-0098-y

Probst, A.J., Weinmaier, T., Raymann, K., Perras, A., Emerson, J.B., Rattei, T., Wanner, G., Klingl, A., Berg, I.A., Yoshinaga, M., Viehweger, B., Hinrichs, K.-U., Thomas, B.C., Meck, S., Auerbach, A.K., Heise, M., Schintlmeister, A., Schmid, M., Wagner, M., Gribaldo, S., Banfield, J.F., Moissl-Eichinger, C., 2014. Biology of a widespread uncultivated archaeon that contributes to carbon fixation in the subsurface. Nature Communications 5, 5497. https://doi.org/10.1038/ncomms6497

Quehenberger, J., Shen, L., Albers, S.-V., Siebers, B., Spadiut, O., 2017. Sulfolobus – A Potential Key Organism in Future Biotechnology. Front Microbiol 8. https://doi.org/10.3389/fmicb.2017.02474

Raymann, K., Brochier-Armanet, C., Gribaldo, S., 2015. The two-domain tree of life is linked to a new root for the Archaea. PNAS 112, 6670–6675. https://doi.org/10.1073/pnas.1420858112

Reysenbach, A.-L., 2001. Class I. Thermoprotei class. nov, in: In DR Boone and RW Castenholz, Eds.. Bergey's Manual of Systematic Bacteriology Volume 1: The Archaea and the Deeply Branching and Phototrophic Bacteria. Springer Verlag, p. 169.

Rinke, C., Schwientek, P., Sczyrba, A., Ivanova, N.N., Anderson, I.J., Cheng, J.-F., Darling, A., Malfatti, S., Swan, B.K., Gies, E.A., Dodsworth, J.A., Hedlund, B.P., Tsiamis, G., Sievert, S.M., Liu, W.-T., Eisen, J.A., Hallam, S.J., Kyrpides, N.C., Stepanauskas, R., Rubin, E.M., Hugenholtz, P., Woyke, T., 2013. Insights into the phylogeny and coding potential of microbial dark matter. Nature advance online publication.

Robinson, D.F., Foulds, L.R., 1981. Comparison of phylogenetic trees. Mathematical Biosciences 53, 131–147. https://doi.org/10.1016/0025-5564(81)90043-2

Segata, N., Börnigen, D., Morgan, X.C., Huttenhower, C., 2013. PhyloPhlAn is a new method for improved phylogenetic and taxonomic placement of microbes. Nat Commun 4, 1–11. https://doi.org/10.1038/ncomms3304

Seitz, K.W., Dombrowski, N., Eme, L., Spang, A., Lombard, J., Sieber, J.R., Teske, A.P., Ettema, T.J.G., Baker, B.J., 2019. Asgard archaea capable of anaerobic hydrocarbon cycling. Nature Communications 10, 1822. https://doi.org/10.1038/s41467-019-09364-x

Seitz, K.W., Lazar, C.S., Hinrichs, K.-U., Teske, A.P., Baker, B.J., 2016. Genomic reconstruction of a novel, deeply branched sediment archaeal phylum with pathways for acetogenesis and sulfur reduction. ISME J 10, 1696–1705. https://doi.org/10.1038/ismej.2015.233

Sieber, C.M.K., Probst, A.J., Sharrar, A., Thomas, B.C., Hess, M., Tringe, S.G., Banfield, J.F., 2018. Recovery of genomes from metagenomes via a dereplication, aggregation and scoring strategy. Nature Microbiology 3, 836–843. https://doi.org/10.1038/s41564-018-0171-1

Sorokin, D.Y., Messina, E., La Cono, V., Ferrer, M., Ciordia, S., Mena, M.C., Toshchakov, S.V., Golyshin, P.N., Yakimov, M.M., 2018. Sulfur Respiration in a Group of Facultatively Anaerobic Natronoarchaea Ubiquitous in Hypersaline Soda Lakes. Front. Microbiol. 9. https://doi.org/10.3389/fmicb.2018.02359

Sorokin, D.Y., Yakimov, M., Messina, E., Merkel, A.Y., Bale, N.J., Sinninghe Damsté, J.S., 2019. Natronolimnobius sulfurireducens sp. nov. and Halalkaliarchaeum desulfuricum gen. nov., sp. nov., the first sulfur-respiring alkaliphilic haloarchaea from hypersaline alkaline lakes. International Journal of Systematic and Evolutionary Microbiology, 69, 2662–2673. https://doi.org/10.1099/ijsem.0.003506

Spang, A., Caceres, E.F., Ettema, T.J.G., 2017. Genomic exploration of the diversity, ecology, and evolution of the archaeal domain of life. Science 357, eaaf3883. https://doi.org/10.1126/science.aaf3883

Spang, A., Saw, J.H., Jørgensen, S.L., Zaremba-Niedzwiedzka, K., Martijn, J., Lind, A.E., van Eijk, R., Schleper, C., Guy, L., Ettema, T.J.G., 2015. Complex archaea that bridge the gap between prokaryotes and eukaryotes. Nature 521, 173–179. https://doi.org/10.1038/nature14447

Stieglmeier, M., Klingl, A., Alves, R.J.E., Rittmann, S.K.-M.R., Melcher, M., Leisch, N., Schleper, C., 2014. Nitrososphaera viennensis gen. nov., sp. nov., an aerobic and mesophilic, ammonia-oxidizing archaeon from soil and a member of the archaeal phylum Thaumarchaeota. International Journal of Systematic and Evolutionary Microbiology 64, 2738–2752. https://doi.org/10.1099/ijs.0.063172-0

Vanwonterghem, I., Evans, P.N., Parks, D.H., Jensen, P.D., Woodcroft, B.J., Hugenholtz, P., Tyson, G.W., 2016. Methylotrophic methanogenesis discovered in the archaeal phylum Verstraetearchaeota. Nature Microbiology 1, 16170. https://doi.org/10.1038/nmicrobiol.2016.170

Wang, H.-C., Minh, B.Q., Susko, E., Roger, A.J., 2018. Modeling Site Heterogeneity with Posterior Mean Site Frequency Profiles Accelerates Accurate Phylogenomic Estimation. Syst Biol 67, 216–235. https://doi.org/10.1093/sysbio/syx068

Wheeler, T.J., Eddy, S.R., 2013. nhmmer: DNA homology search with profile HMMs. Bioinformatics 29, 2487–2489. https://doi.org/10.1093/bioinformatics/btt403

Whitman, W.B., 2016. Modest proposals to expand the type material for naming of prokaryotes. Int. J. Syst. Evol. Microbiol. 66, 2108–2112. https://doi.org/10.1099/ijsem.0.000980

Whitman, W.B., Oren, A., Chuvochina, M., da Costa, M.S., Garrity, G.M., Rainey, F.A., Rossello-Mora, R., Schink, B., Sutcliffe, I., Trujillo, M.E., Ventura, S., 2018. Proposal of the suffix –ota to denote phyla. Addendum to 'Proposal to include the rank of phylum in the International Code of Nomenclature of Prokaryotes.' International Journal of Systematic and Evolutionary Microbiology, 68, 967–969. https://doi.org/10.1099/ijsem.0.002593

Williams, T.A., Szöllősi, G.J., Spang, A., Foster, P.G., Heaps, S.E., Boussau, B., Ettema, T.J.G., Embley, T.M., 2017. Integrative modeling of gene and genome evolution roots the archaeal tree of life. PNAS 114, E4602–E4611. https://doi.org/10.1073/pnas.1618463114

Woese, C.R., Fox, G.E., 1977. Phylogenetic structure of the prokaryotic domain: the primary kingdoms. Proc Natl Acad Sci U S A 74, 5088–5090.

Woese, C.R., Kandler, O., Wheelis, M.L., 1990. Towards a natural system of organisms: proposal for the domains Archaea, Bacteria, and Eucarya. Proc. Natl. Acad. Sci. U.S.A. 87, 4576–4579.

Zaremba-Niedzwiedzka, K., Caceres, E.F., Saw, J.H., Bäckström, D., Juzokaite, L., Vancaester, E., Seitz, K.W., Anantharaman, K., Starnawski, P., Kjeldsen, K.U., Stott, M.B., Nunoura, T., Banfield, J.F., Schramm, A., Baker, B.J., Spang, A., Ettema, T.J.G., 2017. Asgard archaea illuminate the origin of eukaryotic cellular complexity. Nature 541, 353–358. https://doi.org/10.1038/nature21031

Zhou, X., Shen, X.-X., Hittinger, C.T., Rokas, A., 2018. Evaluating Fast Maximum Likelihood-Based Phylogenetic Programs Using Empirical Phylogenomic Data Sets. Mol Biol Evol 35, 486–503. https://doi.org/10.1093/molbev/msx302

Zuo, G., Xu, Z., Hao, B., 2015. Phylogeny and Taxonomy of Archaea: A Comparison of the Whole-Genome-Based CVTree Approach with 16S rRNA Sequence Analysis. Life 5, 949–968. https://doi.org/10.3390/life5010949

824 # Tables and Figures

825 **Table 1 | Correspondence between GTDB and NCBI taxonomy.** Named GTDB phyla, major classes and
826 selected orders are listed with their corresponding NCBI taxonomy. Note that, in cases where GTDB and
827 NCBI lineages are not an exact match, the NCBI lineage with the highest number of matching taxa is provided.
828 Abbreviations: n.a. = not assigned, meaning no rank has been assigned to this lineage in the NCBI taxonomy.
829 Further details regarding the correspondence between NCBI and GTDB taxa are provided in Table S23 and
830 S24.
831

GTDB phylum	GTDB class; order	NCBI phylum	NCBI class
p__Halobacteriota	c__Archaeoglobi	Euryarchaeota	Archaeoglobi
p__Halobacteriota	c__Halobacteria	Euryarchaeota	Halobacteria
p__Halobacteriota	c__Methanomicrobia	Euryarchaeota	Methanomicrobia
p__Halobacteriota	c__Methanonatronarchaeia	Euryarchaeota	Methanonatronarchaeia
p__Halobacteriota	c__Methanosarcinia	Euryarchaeota	Methanomicrobia
p__Thermoplasmatota	c__E2	Euryarchaeota	Thermoplasmata
p__Thermoplasmatota	c__Poseidoniia	Euryarchaeota	n.a.
p__Thermoplasmatota	c__Thermoplasmata	Euryarchaeota	Thermoplasmata
p__Methanobacteriota	c__Methanobacteria	Euryarchaeota	Methanobacteria
p__Methanobacteriota	c__Methanococci	Euryarchaeota	Methanococci
p__Methanobacteriota	c__Methanopyri	Euryarchaeota	Methanopyri
p__Methanobacteriota	c__Thermococci	Euryarchaeota	Thermococci
p__Hadarchaeota	c__Hadarchaeia	Euryarchaeota	Hadesarchaea
p__Hydrothermarchaeota	c__Hydrothermarchaeia	Euryarchaeota	n.a.
p__Thermoproteota	c__Bathyarchaeia	Ca. Bathyarchaeota	n.a.
p__Thermoproteota	c__Korarchaeia	Ca. Korarchaeota	n.a.
p__Thermoproteota	c__Methanomethylicia	Ca. Verstraetearchaeota	n.a.
p__Thermoproteota	c__Nitrososphaeria	Thaumarchaeota	n.a.
p__Thermoproteota	c__Nitrososphaeria; o__Caldarchaeales[1]	Thaumarchaeota	n.a.
p__Thermoproteota	c__Thermoproteia	Crenarchaeota	Thermoprotei
p__Thermoproteota	c__Thermoproteia; o__Gearchaeales[2]	Crenarchaeota	n.a.
p__Asgardarchaeota	c__Heimdallarchaeia	Ca. Heimdallarchaeota	n.a.
p__Asgardarchaeota	c__Lokiarchaeia	Ca. Lokiarchaeota	n.a.
p__Asgardarchaeota	c__Lokiarchaeia; o__Helarchaeales	Ca. Helarchaeota	n.a.
p__Asgardarchaeota	c__Lokiarchaeia; o__Odinarchaeales	Ca. Odinarchaeota	n.a.
p__Nanoarchaeota	c__Nanoarchaeia	Ca. Woesearchaeota/ Ca. Nanoarchaeota	n.a.
p__Nanoarchaeota	c__Nanoarchaeia; o__Pacearchaeales[3]	n.a.	n.a.
p__Nanoarchaeota	c__Nanoarchaeia; o__Parvarchaeales	Ca. Parvarchaeota	n.a.
p__Nanoarchaeota	c__Nanoarchaeia; o__Woesearchaeales[4]	n.a.	n.a.
p__Nanohaloarchaeota	c__Nanohaloarchaea	Euryarchaeota	Nanohaloarchaea
p__Nanohaloarchaeota	c__Nanosalinia	Euryarchaeota	Nanohaloarchaea
p__Aenigmarchaeota[5]	c__Aenigmarchaeia[5]	Ca. Aenigmarchaeota	n.a.
p__Micrarchaeota	c__Micrarchaeia	Ca. Micrarchaeota	n.a.
p__Iainarchaeota	c__Iainarchaeia	Ca. Diapherotrites	n.a.

p__Altarchaeota	c__Altarchaeia	Ca. Altiarchaeota	n.a.
p__Huberarchaeota	c__Huberarchaeia	Ca. Huberarchaea	n.a.

[1] proposed as "Candidatus Aigarchaeota" (Nunoura et al. 2011)
[2] proposed as "Candidatus Geoarchaeota" Kozubal et al. 2013". Note, name will be corrected to "o__Gearchaeales" in subsequent GTDB releases.
[3] proposed as "Candidatus Pacearchaeota" (Castelle et al. 2015)
[4] proposed as "Candidatus Woesearchaeota" (Castelle et al. 2015)
[5] name will be corrected to "Aenigmatarchae*" in subsequent GTDB releases.

Figure 1 | Comparison of rank normalized archaeal GTDB and NCBI taxonomies. (a) Relative evolutionary divergence (RED) of taxa defined by the NCBI taxonomy; **(b)** RED of taxa defined by the curated GTDB taxonomy (04-RS89). In (a) and (b) each data point (black circle) represents a taxon distributed according to its RED value (x-axis) and its rank (y-axis). The fill colours of the circle (blue, grey, or orange) indicate that a taxon is monophyletic, operationally monophyletic (defined as having an F measure >0.95), or polyphyletic, respectively in the underlying genome tree. An overlaid histogram shows the relative abundance of monophyletic, operationally monophyletic, and polyphyletic taxa for each 0.025 RED interval. A blue bar shows the median RED value, and two black bars the RED interval (+/- 0.1) for each rank. Note, that in the NCBI taxonomy the values of the higher ranks (order and above) are very unevenly distributed, to the point where the median distributions are not even in the expected order, i.e. the median RED value for classes was higher than the median order value. The GTDB taxonomy uses the RED value to resolve over- and under-classified taxa by moving them to a new interior node (horizontal shift in plot) or by assigning them to a new rank (vertical shift in plot). Only monophyletic or operationally monophyletic taxa were used to calculate the median RED values for each rank. In addition, only taxa with a minimum of two children (e.g. a phylum with two or more classes, or a class with two or more orders) were considered for the GTDB tree (--min_children 2), however, a more lenient approach (--min_children 0) was necessary for the NCBI tree since, except for the Euryarchaeota, none of the other NCBI phyla had the required minimum of two classes. Note, that the NCBI phylum Crenarchaeota is not displayed in the NCBI plot, since all genomes in this NCBI phylum are assigned to the class Thermoprotei, resulting in a single node decorated as "p__Crenarchaeota; c__Thermoprotei" (Tpr). Also, Korarchaeota are only represented by a single species, Korarchaeum cryptofilum, in r89 and hence there is no internal node to be displayed in this plot. RED values were calculated based on the ar122.r89 tree, inferred from 122 concatenated proteins, decorated with the NCBI and GTDB taxonomy, respectively. **(c)** Rank comparison of GTDB and NCBI taxonomies. Shown are changes in GTDB compared to the NCBI taxonomic assignments across 2,392 archaeal genomes from RefSeq/GenBank release 89. In the bars on the left, a taxon is shown as unchanged if its name was identical in both taxonomies, as a passive change if the GTDB taxonomy provided name information absent in the NCBI taxonomy (missing names), or as active change if the name was different between the two taxonomies. The right bar shows the changes of the entire tax string (consisting of seven ranks) per genome, indicating that most genomes had active and passive changes in their taxonomy. See Suppl. Text for more details.

Figure 2 | Comparison of marker sets, inference methods and models. Phylogenetic trees inferred with different methods, from varying concatenated alignments, or via supertree approaches were decorated with the GTDB 04-RS89 taxonomy. RED distributions for taxa at each rank (p, phylum; c, class; o, order; f, family; g, genus) are shown relative to the median RED value of the rank. The legend indicates the percentage of polyphyletic taxa per rank, defined as an F measure <0.95. Note that only taxa with two or more genomes were included. **(a)** trees inferred with IQ-TREE from a concatenated alignment of the 122 GTDB markers with ~5,000 alignment columns using different profile mixture models (C10 PMSF, C10, C60), and from the untrimmed alignment 32kAA alignment. **(b)** Trees inferred from a modified concatenated alignment of the 122 GTDB markers to account for compositional bias, including stationary (BMGE) and progressive trimming (Tr. 20%, Tr. 40%) of heterogeneous sites, and clustering of sites with shared homology (Divvier). **(c)** Trees inferred from a modified concatenated alignment of the 122 GTDB markers including recoding into 4

character-states (C60 SR4), recoding and stationary trimming (BMGE C60 SR4), and removal of 20% and 40% of the fastest evolving sites (SlowFaster 20% and 40%). Note that, due to technical limitations a reduced order-dereplicated genome set was used for SlowFaster, allowing the evaluation of the ranks phylum and class only. **(d)** Trees inferred from 122 marker alignments using different inference software and models, including FastTree2, ExaML, and Phylobayes Note due to computational constrains PhyloBayes was calculated from the order dereplicated data set, allowing the evaluation of the ranks phylum and class only. (**e)** Trees inferred from alternative markers, including 16 ribosomal proteins (rp1), 23 ribosomal proteins (rp2), SSU rRNA genes (SSU), and a set of 53 marker proteins (ar53).
(f) Trees inferred with the ASTRAL supertree approach using 122 and 253 marker proteins. More details about inference models and methods are given in **Table S10**. The number in square brackets following each tree name, e.g. [2.1] refers to the number of this tree in the supplements, including Table S10.

Figure 3 | Impact of different rooting scenarios on the relative evolutionary divergence (RED). The rooting approach implemented in GTDB **(a),** which calculates the relative evolutionary divergence (RED) as the median of all possible rootings of phyla with at least two classes (red arrows), is compared to a fixed root between the DPANN superphylum (red arrow) and the remaining Archaea **(b)**, and to a fixed root within the NCBI phylum Euryarchatoa, which translates to a root between the two phyla Thermoplasmata and Halobacteriota (red arrow) and the rest of the Archaea in the GTDB taxonomy **(c)**. In the upper RED plot each data point (black circle) represents a taxon distributed according to its RED value (x-axis) and its rank (y-axis). An overlaid histogram shows the relative abundance of taxa for each 0.025 RED interval, a blue bar shows the median RED value, and two black bars the RED interval (+/- 0.1) for each rank. Note that, overall, the ranks can be distinguished based on their RED value, regardless of the applied rooting scenario. Furthermore, RED values are relative and should not be directly compared between plots as they are dataset specific. Rather, the distribution of RED values, i.e. the distance (positive or negative) from the median of the RED value for each rank (ΔRED) is the key metric. The trees include a label highlighting the corresponding NCBI phylum Euryarchaeota (Eury), as a point of reference. The scale bars indicate 0.1 substitutions.

Figure 4 | Rank normalized archaeal GTDB taxonomy. Species dereplicated scaled ar122.r89 tree decorated with the archaeal GTDB taxonomy R04-RS89. The outer blue ring denotes the rank normalized phyla, and the light blue clades indicate the classes in the rank normalized GTDB taxonomy. Classes with 10 or more taxa are labelled, and a below class divergence is indicated by providing the lower rank (e.g. order) for a given class. The two GTDB phyla consisting of only a single species each, namely Huberarchaeota and EX4484-52 are highlighted by red branches indicating their uncertain placement in the ar122.r89 tree. The inner orange ring denotes the r89 NCBI phyla with 2 or more taxa. The NCBI superphyla TACK and DPANN are indicated with gray color strips. Abbreviations are the following: Bat (*Ca.* Bathyarchaeota), M (*Ca.* Marsarchaeota), V (*Ca.* Verstraetearchaeota), T (*Ca*. Thorarchaeota), L (*Ca*. Lokiarchaeota), H (*Ca.* Heimdallarchaeota), Woe (*Ca.* Woesearchaeota), P (Ca. Parvarchaeota), N (Nanoarchaeota), Nh (*Ca.* Nanohaloarchaeota), A (*Ca*. Aenigmarchaeota), M (*Ca.* Micrarchaeota), D (*Ca*. Diapherotrites). Note: the scaled tree was generated by replacing the branch lengths with the median relative evolutionary distance (RED), calculated across all plausible rootings. Bootstrap values over 90% are indicated by blue dots. Scale bar indicates 0.1 RED.

Figure 5 | Reclassification of the members of the Thaumarchaeota. Cladogram based on the ar122.r89 reference tree showing the GTDB phylum Thermoproteota; with the classes Korarchaeia, Thermoprotei, Methanomethylicia (former phylum *Candidatus* Verstraetearchaeota), Bathyarchaeia, and Nitrososphaeria. The validly published class Nitrososphaeria (light blue) was emended in GTDB to include all taxa assigned to the phylum Thaumarchaeota in the NCBI r89 taxonomy. The type species of this lineage is *Nitrososphaera viennensis* (Stieglmeier et al. 2014), which serves as the type for higher taxa including the genus *Nitrososphaera*, the family *Nitrososphaeraceae*, the order *Nitrososphaerales*, and the class *Nitrososphaeria*.

The genome of the *Nitrososphaera viennensis* type strain EN76^T (=DSM 26422^T=JMC 19564^T), is highlighted in white. Arrow points to outgroup.

Supplementary information

Supplementary Tables and Figures

See files "*Supplementary Tables" 1 and 2, and "Supplementary Figures*".

Supplementary data

All GTDB files for Release 04-RS89 are available through the GTDB repository https://data.ace.uq.edu.au/public/gtdb/data/releases/release89/89.0/

Supplementary File 01 | Phylogenetic trees. Newick files of all GTDB decorated trees: *Suppl_file_01_trees_4_paper.zip*

Supplementary File 02 | SR4 model used for data recoded inferences. File name: **.nex*

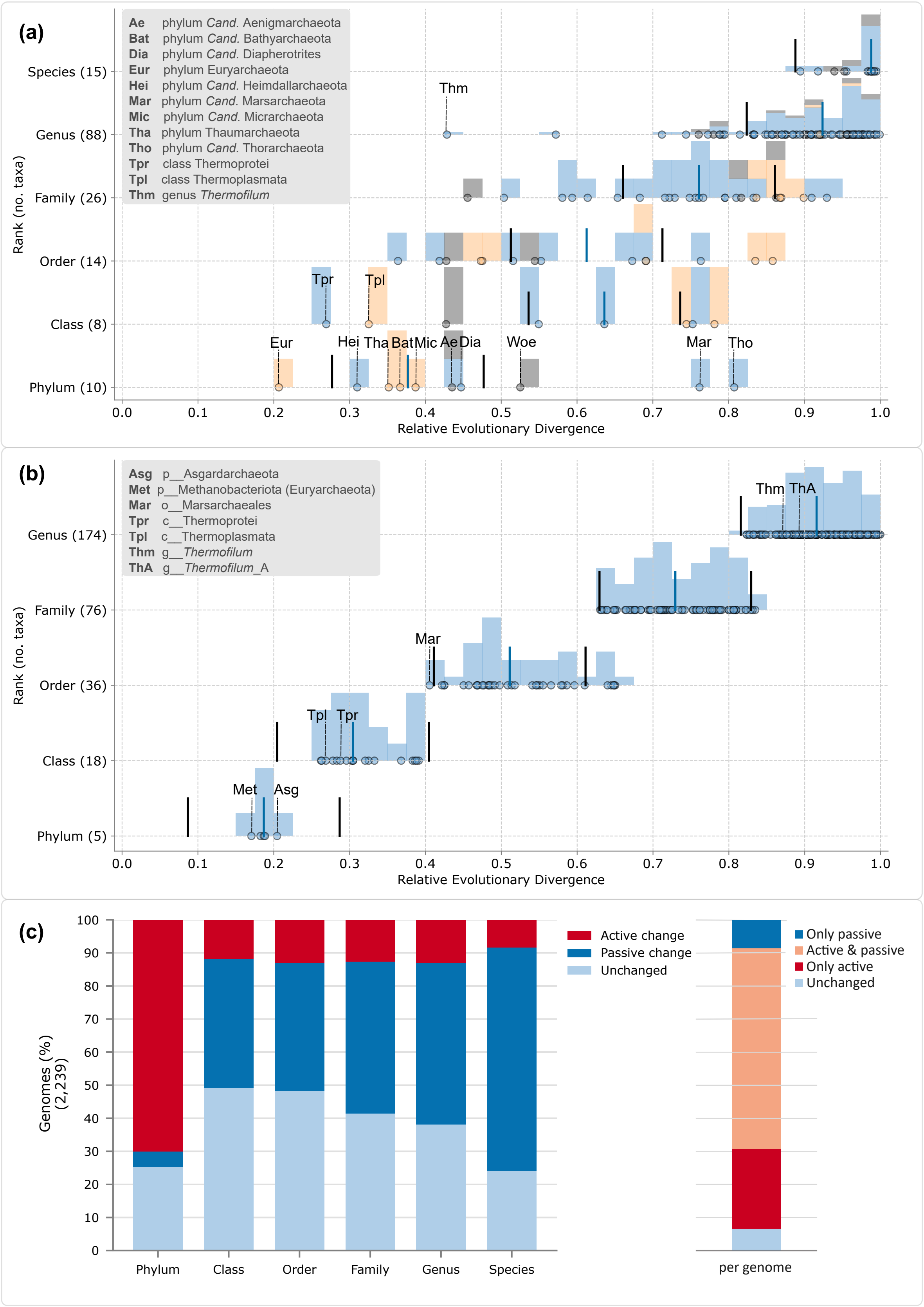
(a)
Ae phylum Cand. Aenigmarchaeota
Bat phylum Cand. Bathyarchaeota
Dia phylum Cand. Diapherotrites
Eur phylum Euryarchaeota
Hei phylum Cand. Heimdallarchaeota
Mar phylum Cand. Marsarchaeota
Mic phylum Cand. Micrarchaeota
Tha phylum Thaumarchaeota
Tho phylum Cand. Thorarchaeota
Tpr class Thermoprotei
Tpl class Thermoplasmata
Thm genus Thermofilum
Species (15)
Genus (88)
Family (26)
Order (14)
Class (8)
Phylum (10)
Rank (no. taxa)
Thm
Tpr
Tpl
Eur
Hei
Tha
Bat
Mic
Ae
Dia
Woe
Mar
Tho
0.0
0.1
0.2
0.3
0.4
0.5
0.6
0.7
0.8
0.9
1.0
Relative Evolutionary Divergence
(b)
Asg p__Asgardarchaeota
Met p__Methanobacteriota (Euryarchaeota)
Mar o__Marsarchaeales
Tpr c__Thermoprotei
Tpl c__Thermoplasmata
Thm g__Thermofilum
ThA g__Thermofilum_A
Genus (174)
Family (76)
Order (36)
Class (18)
Phylum (5)
Rank (no. taxa)
Thm
ThA
Mar
Tpl
Tpr
Met
Asg
0.0
0.1
0.2
0.3
0.4
0.5
0.6
0.7
0.8
0.9
1.0
Relative Evolutionary Divergence
(c)
Genomes (%) (2,239)
100
90
80
70
60
50
40
30
20
10
0
Phylum
Class
Order
Family
Genus
Species
Active change
Passive change
Unchanged
Only passive
Active & passive
Only active
Unchanged
per genome

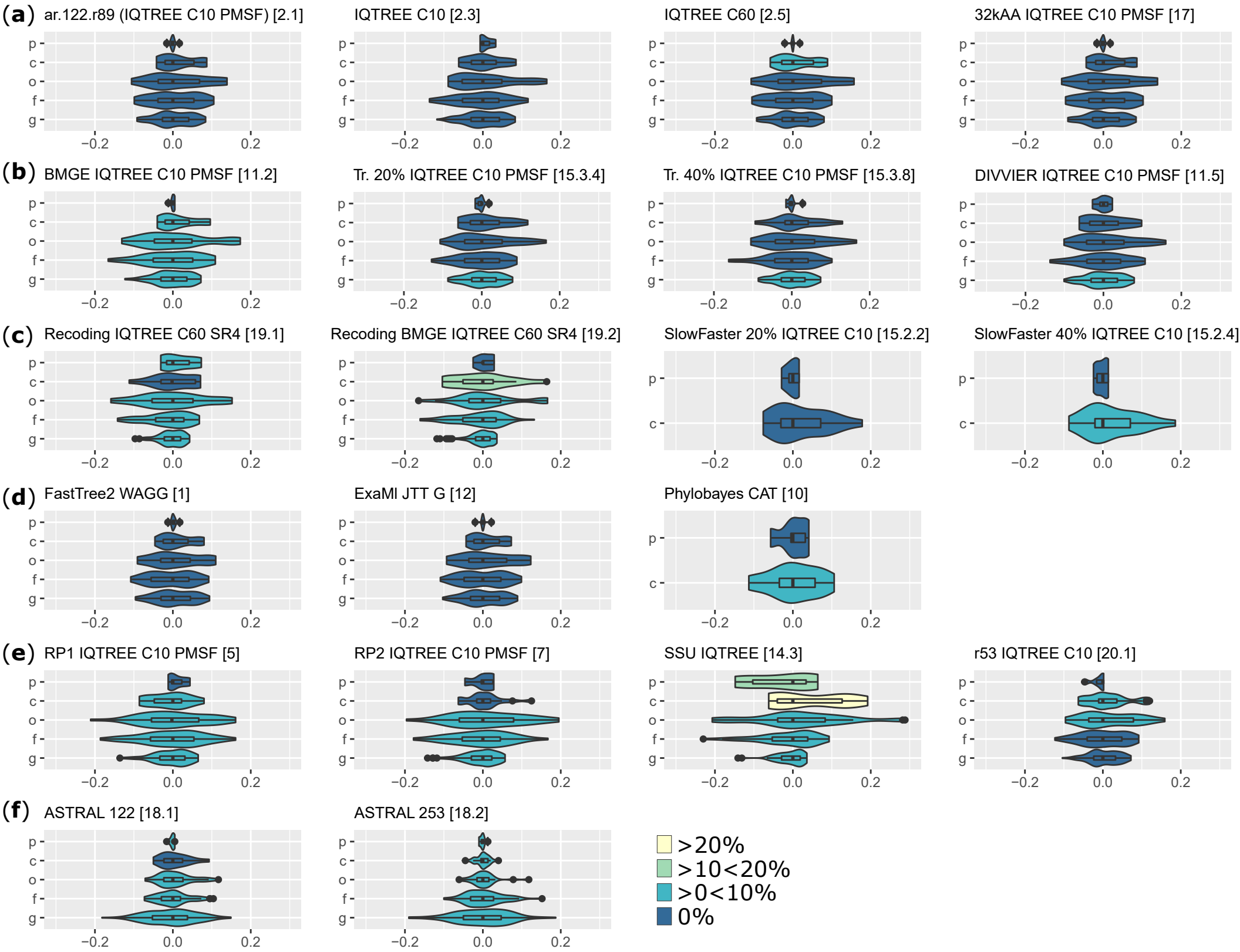
(a)
ar.122.r89 (IQTREE C10 PMSF) [2.1]
IQTREE C10 [2.3]
IQTREE C60 [2.5]
32kAA IQTREE C10 PMSF [17]
(b)
BMGE IQTREE C10 PMSF [11.2]
Tr. 20% IQTREE C10 PMSF [15.3.4]
Tr. 40% IQTREE C10 PMSF [15.3.8]
DIVVIER IQTREE C10 PMSF [11.5]
(c)
Recoding IQTREE C60 SR4 [19.1]
Recoding BMGE IQTREE C60 SR4 [19.2]
SlowFaster 20% IQTREE C10 [15.2.2]
SlowFaster 40% IQTREE C10 [15.2.4]
(d)
FastTree2 WAGG [1]
ExaMl JTT G [12]
Phylobayes CAT [10]
(e)
RP1 IQTREE C10 PMSF [5]
RP2 IQTREE C10 PMSF [7]
SSU IQTREE [14.3]
r53 IQTREE C10 [20.1]
(f)
ASTRAL 122 [18.1]
ASTRAL 253 [18.2]
p
c
o
f
g
−0.2
0.0
0.2
>20%
>10<20%
>0<10%
0%

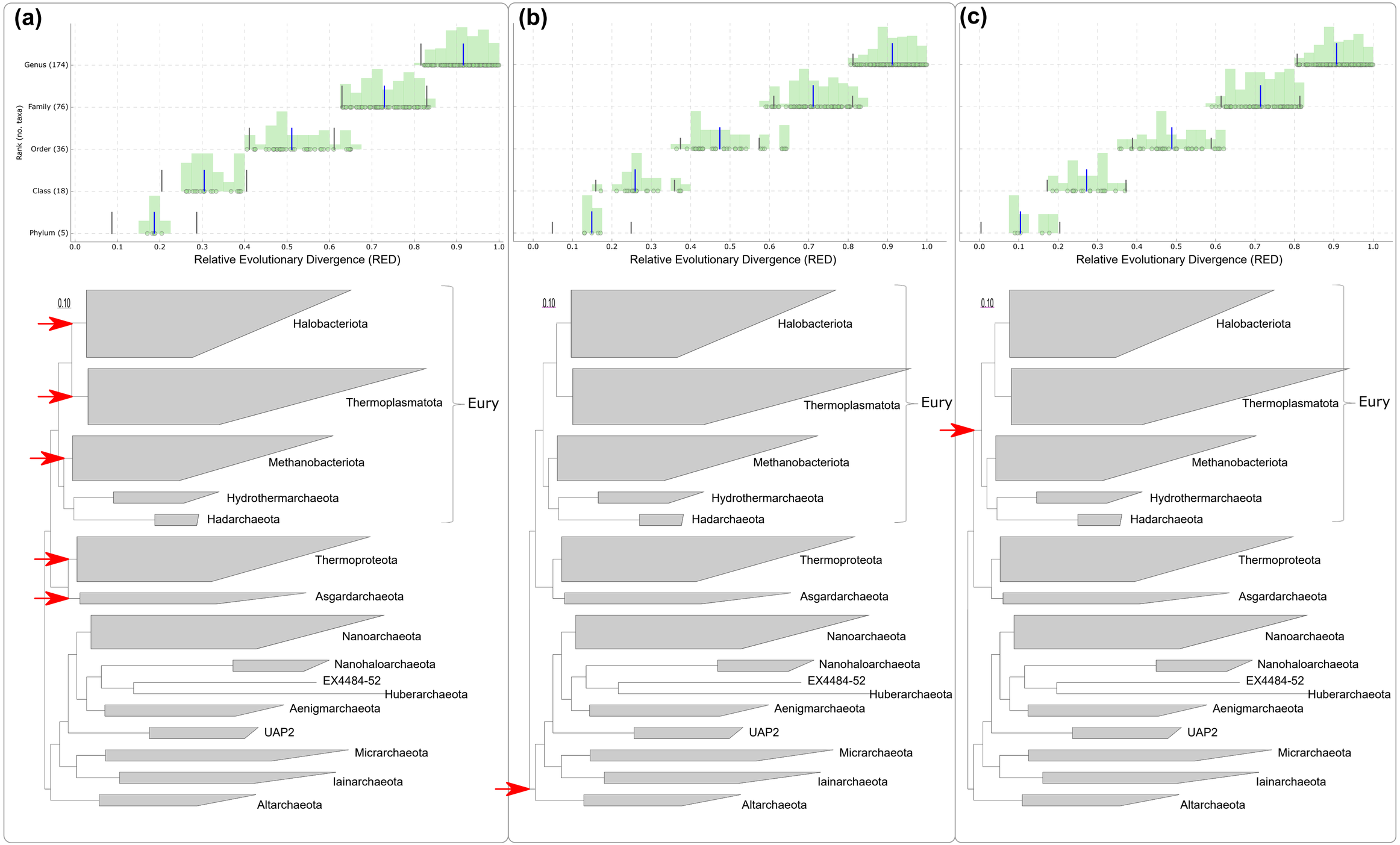
(a)
(b)
(c)
Genus (174)
Family (76)
Order (36)
Class (18)
Phylum (5)
Rank (no. taxa)
0.0 0.1 0.2 0.3 0.4 0.5 0.6 0.7 0.8 0.9 1.0
Relative Evolutionary Divergence (RED)
0.10
Halobacteriota
Thermoplasmatota
Methanobacteriota
Hydrothermarchaeota
Hadarchaeota
Eury
Thermoproteota
Asgardarchaeota
Nanoarchaeota
Nanohaloarchaeota
EX4484-52
Huberarchaeota
Aenigmarchaeota
UAP2
Micrarchaeota
Iainarchaeota
Altarchaeota

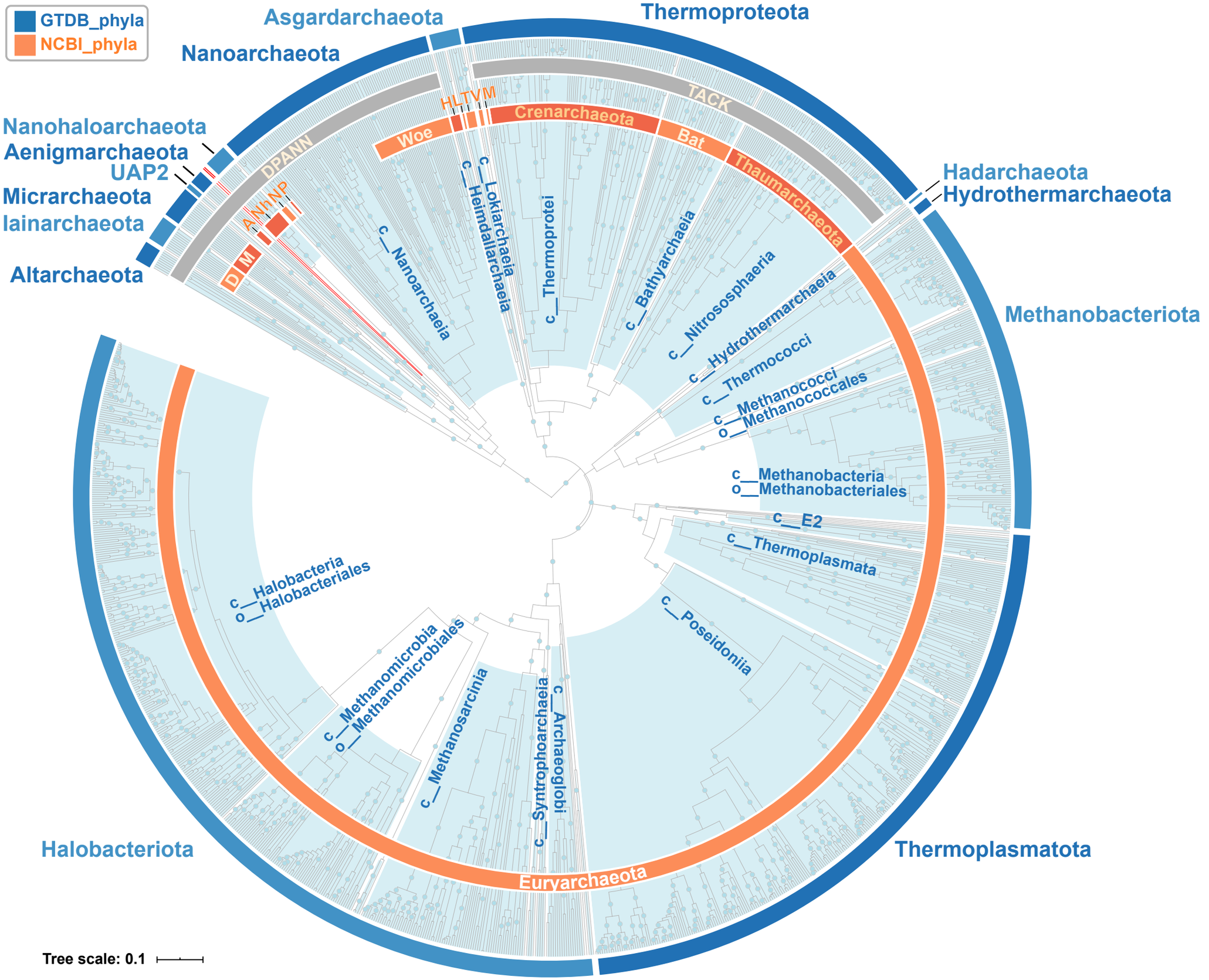
GTDB_phyla
NCBI_phyla
Asgardarchaeota
Thermoproteota
Nanoarchaeota
Nanohaloarchaeota
Aenigmarchaeota
UAP2
Micrarchaeota
Iainarchaeota
Altarchaeota
DPANN
TACK
HLTVM
Crenarchaeota
Woe
Bat
Thaumarchaeota
AnhNP
DM
Hadarchaeota
Hydrothermarchaeota
Methanobacteriota
c__Nanoarchaeia
c__Lokiarchaeia
c__Heimdallarchaeia
c__Thermoprotei
c__Bathyarchaeia
c__Nitrososphaeria
c__Hydrothermarchaeia
c__Thermococci
c__Methanococci
o__Methanococcales
c__Methanobacteria
o__Methanobacteriales
c__E2
c__Thermoplasmata
c__Poseidoniia
c__Halobacteria
o__Halobacteriales
c__Methanomicrobia
o__Methanomicrobiales
c__Methanosarcinia
c__Syntrophoarchaeia
c__Archaeoglobi
Halobacteriota
Euryarchaeota
Thermoplasmatota
Tree scale: 0.1

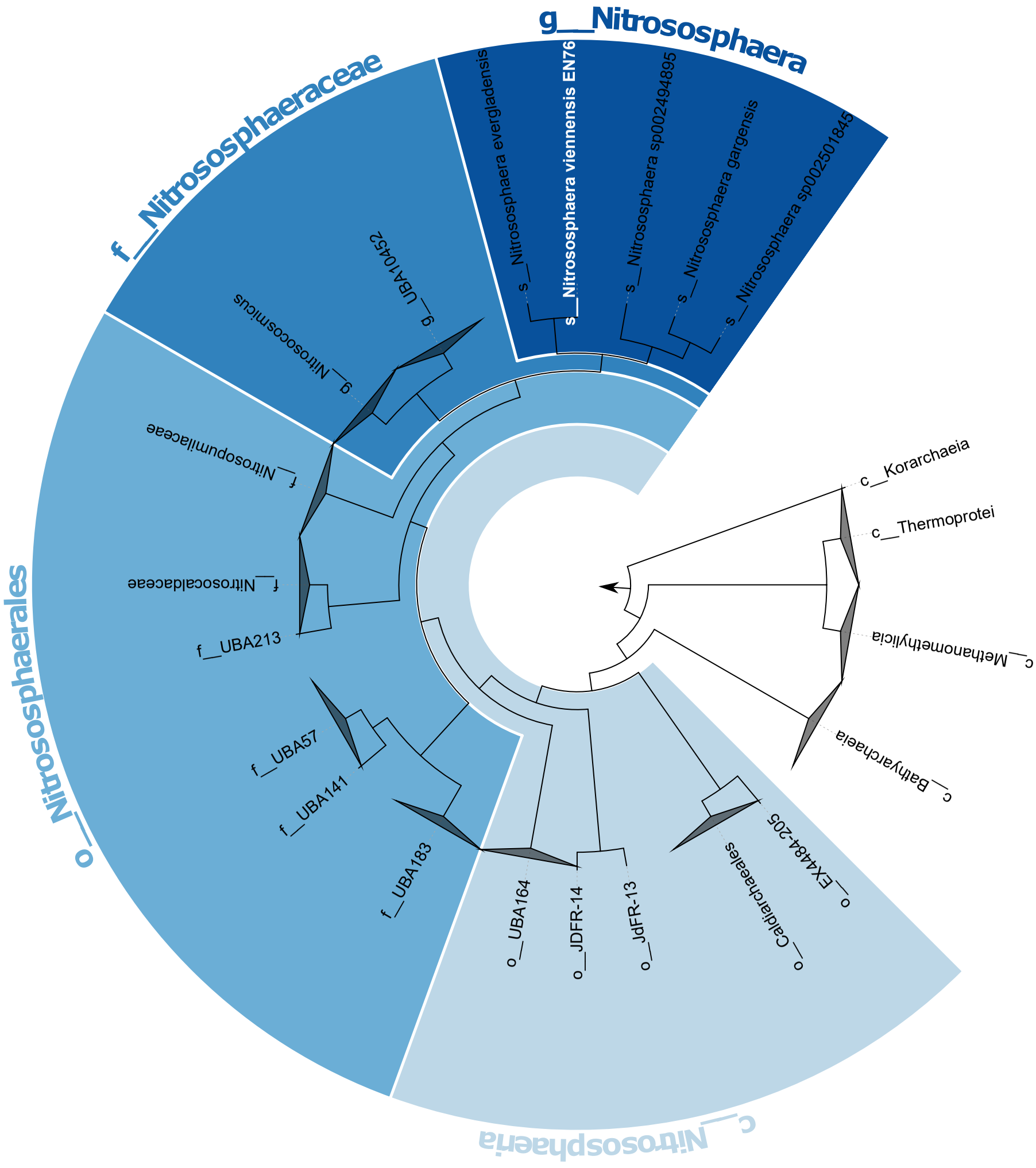
g__Nitrososphaera
s__Nitrososphaera evergladensis
s__Nitrososphaera viennensis EN76
s__Nitrososphaera sp002494895
s__Nitrososphaera gargensis
s__Nitrososphaera sp002501845
f__Nitrososphaeraceae
g__UBA10452
g__Nitrososcosmicus
f__Nitrosopumilaceae
f__Nitrosocaldaceae
f__UBA213
f__UBA57
f__UBA141
f__UBA183
o__Nitrososphaerales
o__UBA164
o__JDFR-14
o__JdFR-13
o__Caldiarchaeales
o__EX4484-205
c__Bathyarchaeia
c__Methanomethylicia
c__Thermoprotei
c__Korarchaeia
c__Nitrososphaeria

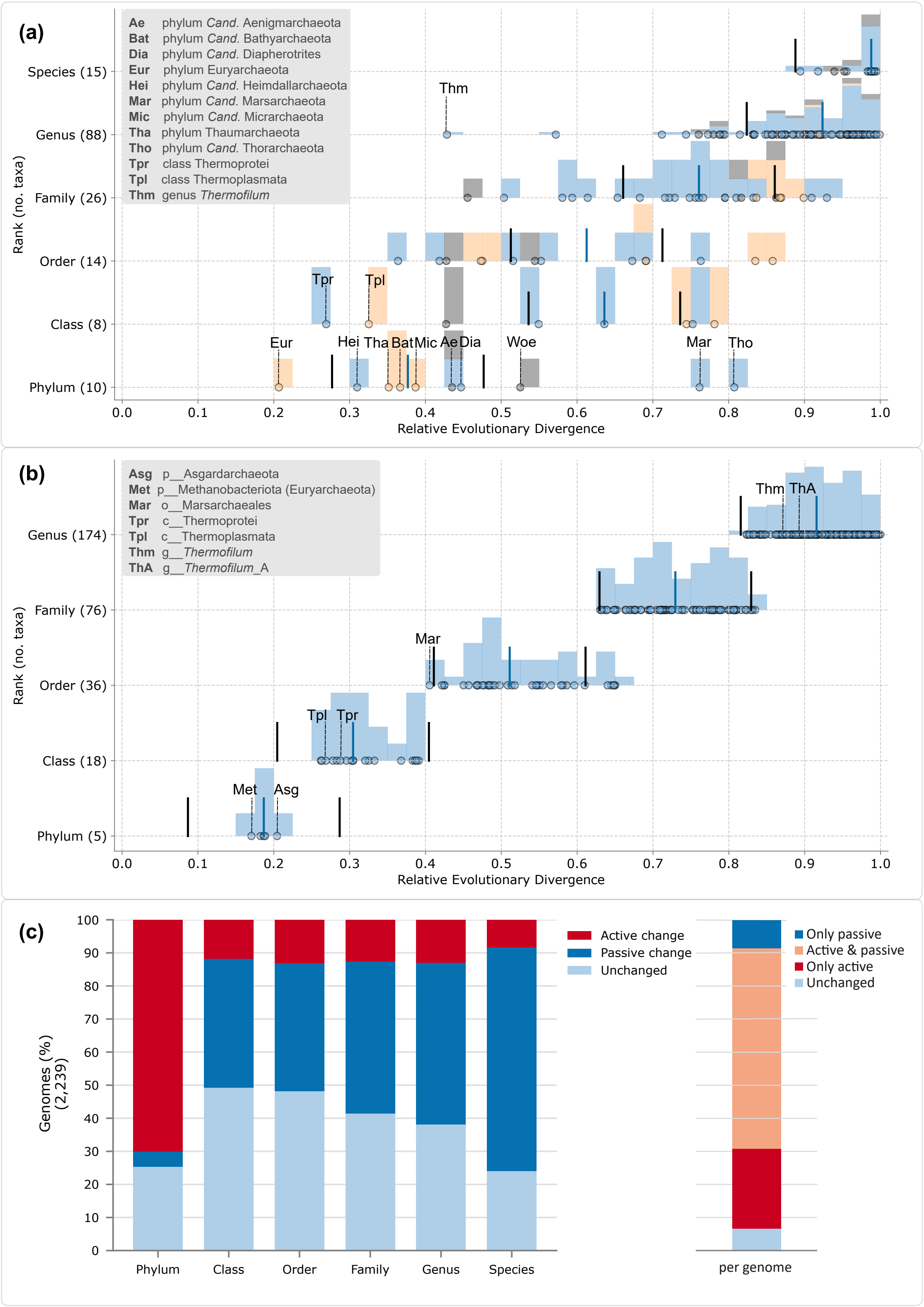
(a)
Ae phylum Cand. Aenigmarchaeota
Bat phylum Cand. Bathyarchaeota
Dia phylum Cand. Diapherotrites
Eur phylum Euryarchaeota
Hei phylum Cand. Heimdallarchaeota
Mar phylum Cand. Marsarchaeota
Mic phylum Cand. Micrarchaeota
Tha phylum Thaumarchaeota
Tho phylum Cand. Thorarchaeota
Tpr class Thermoprotei
Tpl class Thermoplasmata
Thm genus Thermofilum
Species (15)
Genus (88)
Family (26)
Order (14)
Class (8)
Phylum (10)
Rank (no. taxa)
Thm
Tpr
Tpl
Eur
Hei
Tha
Bat
Mic
Ae
Dia
Woe
Mar
Tho
0.0
0.1
0.2
0.3
0.4
0.5
0.6
0.7
0.8
0.9
1.0
Relative Evolutionary Divergence
(b)
Asg p__Asgardarchaeota
Met p__Methanobacteriota (Euryarchaeota)
Mar o__Marsarchaeales
Tpr c__Thermoprotei
Tpl c__Thermoplasmata
Thm g__Thermofilum
ThA g__Thermofilum_A
Genus (174)
Family (76)
Order (36)
Class (18)
Phylum (5)
Rank (no. taxa)
Thm
ThA
Mar
Tpl
Tpr
Met
Asg
0.0
0.1
0.2
0.3
0.4
0.5
0.6
0.7
0.8
0.9
1.0
Relative Evolutionary Divergence
(c)
Genomes (%) (2,239)
100
90
80
70
60
50
40
30
20
10
0
Phylum
Class
Order
Family
Genus
Species
Active change
Passive change
Unchanged
Only passive
Active & passive
Only active
Unchanged
per genome

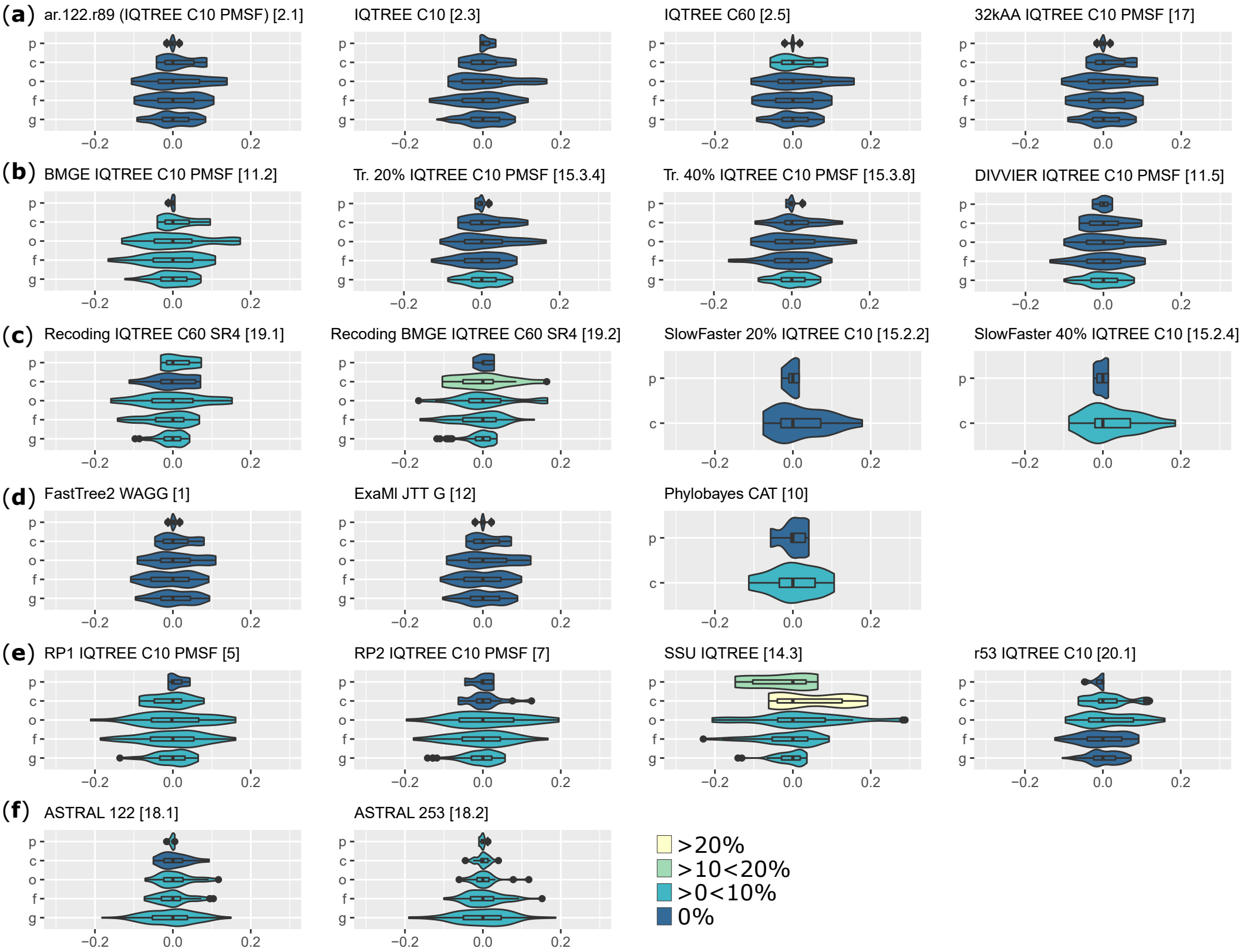
(a)
ar.122.r89 (IQTREE C10 PMSF) [2.1]
IQTREE C10 [2.3]
IQTREE C60 [2.5]
32kAA IQTREE C10 PMSF [17]
(b)
BMGE IQTREE C10 PMSF [11.2]
Tr. 20% IQTREE C10 PMSF [15.3.4]
Tr. 40% IQTREE C10 PMSF [15.3.8]
DIVVIER IQTREE C10 PMSF [11.5]
(c)
Recoding IQTREE C60 SR4 [19.1]
Recoding BMGE IQTREE C60 SR4 [19.2]
SlowFaster 20% IQTREE C10 [15.2.2]
SlowFaster 40% IQTREE C10 [15.2.4]
(d)
FastTree2 WAGG [1]
ExaMl JTT G [12]
Phylobayes CAT [10]
(e)
RP1 IQTREE C10 PMSF [5]
RP2 IQTREE C10 PMSF [7]
SSU IQTREE [14.3]
r53 IQTREE C10 [20.1]
(f)
ASTRAL 122 [18.1]
ASTRAL 253 [18.2]
p
c
o
f
g
−0.2
0.0
0.2
>20%
>10<20%
>0<10%
0%

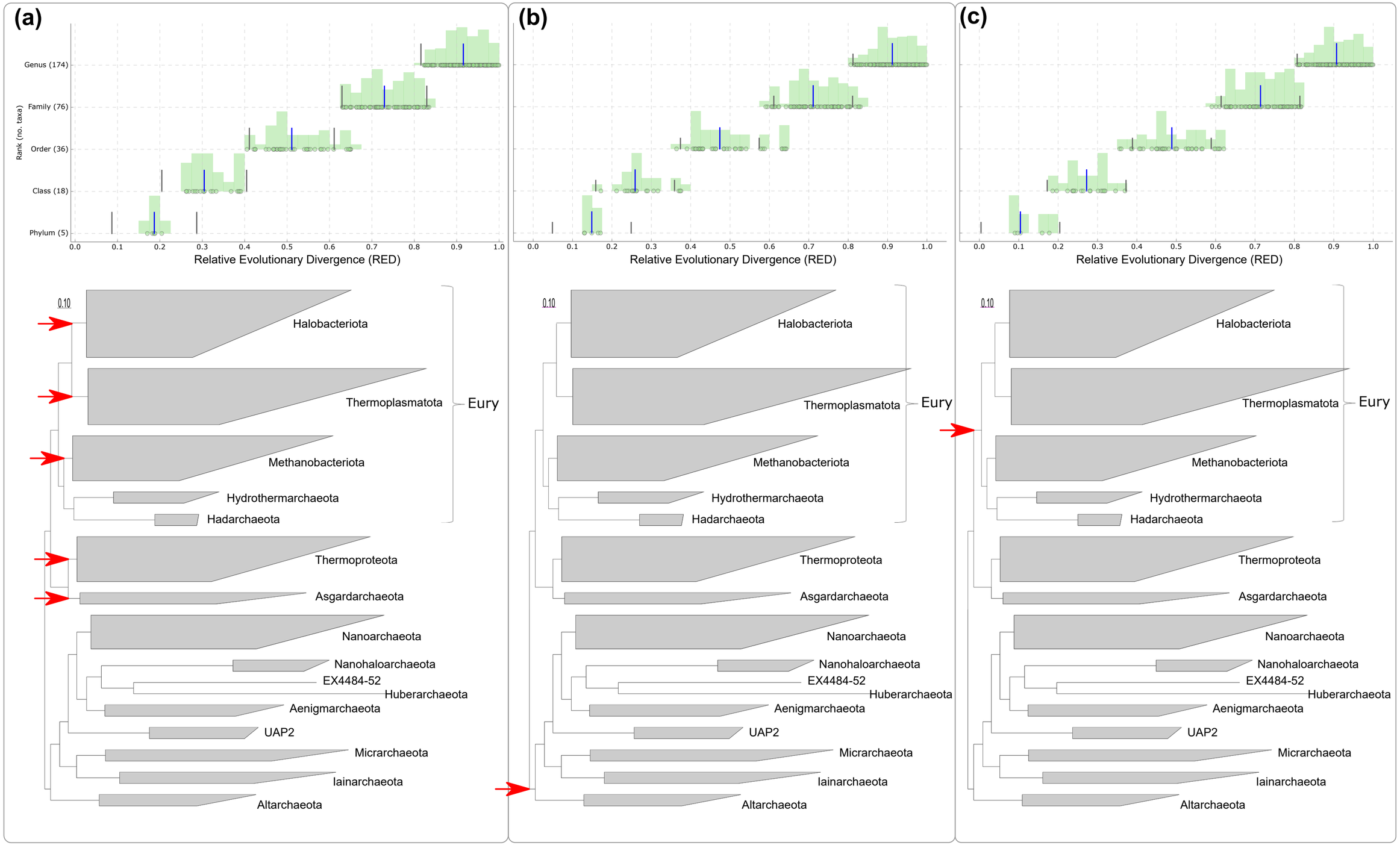
(a)
(b)
(c)
Genus (174)
Family (76)
Order (36)
Class (18)
Phylum (5)
Rank (no. taxa)
0.0 0.1 0.2 0.3 0.4 0.5 0.6 0.7 0.8 0.9 1.0
Relative Evolutionary Divergence (RED)
0.10
Halobacteriota
Thermoplasmatota
Methanobacteriota
Hydrothermarchaeota
Hadarchaeota
Eury
Thermoproteota
Asgardarchaeota
Nanoarchaeota
Nanohaloarchaeota
EX4484-52
Huberarchaeota
Aenigmarchaeota
UAP2
Micrarchaeota
Iainarchaeota
Altarchaeota

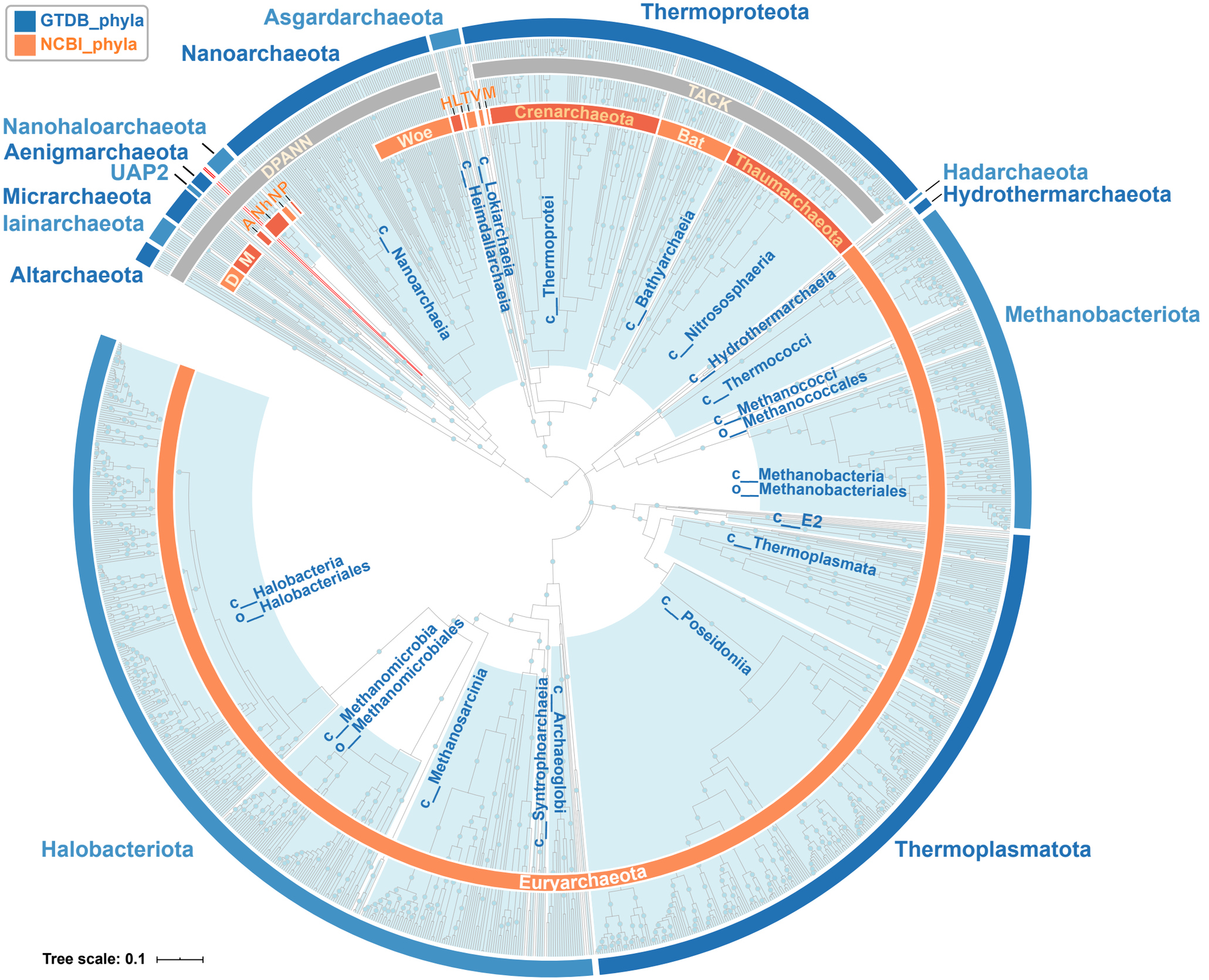
GTDB_phyla
NCBI_phyla
Asgardarchaeota
Thermoproteota
Nanoarchaeota
Nanohaloarchaeota
Aenigmarchaeota
UAP2
Micrarchaeota
Iainarchaeota
Altarchaeota
DPANN
TACK
HLTVM
Crenarchaeota
Woe
Bat
Thaumarchaeota
AnhNP
DM
Hadarchaeota
Hydrothermarchaeota
Methanobacteriota
c__Nanoarchaeia
c__Lokiarchaeia
c__Heimdallarchaeia
c__Thermoprotei
c__Bathyarchaeia
c__Nitrososphaeria
c__Hydrothermarchaeia
c__Thermococci
c__Methanococci
o__Methanococcales
c__Methanobacteria
o__Methanobacteriales
c__E2
c__Thermoplasmata
c__Poseidoniia
c__Halobacteria
o__Halobacteriales
c__Methanomicrobia
o__Methanomicrobiales
c__Methanosarcinia
c__Syntrophoarchaeia
c__Archaeoglobi
Halobacteriota
Euryarchaeota
Thermoplasmatota
Tree scale: 0.1

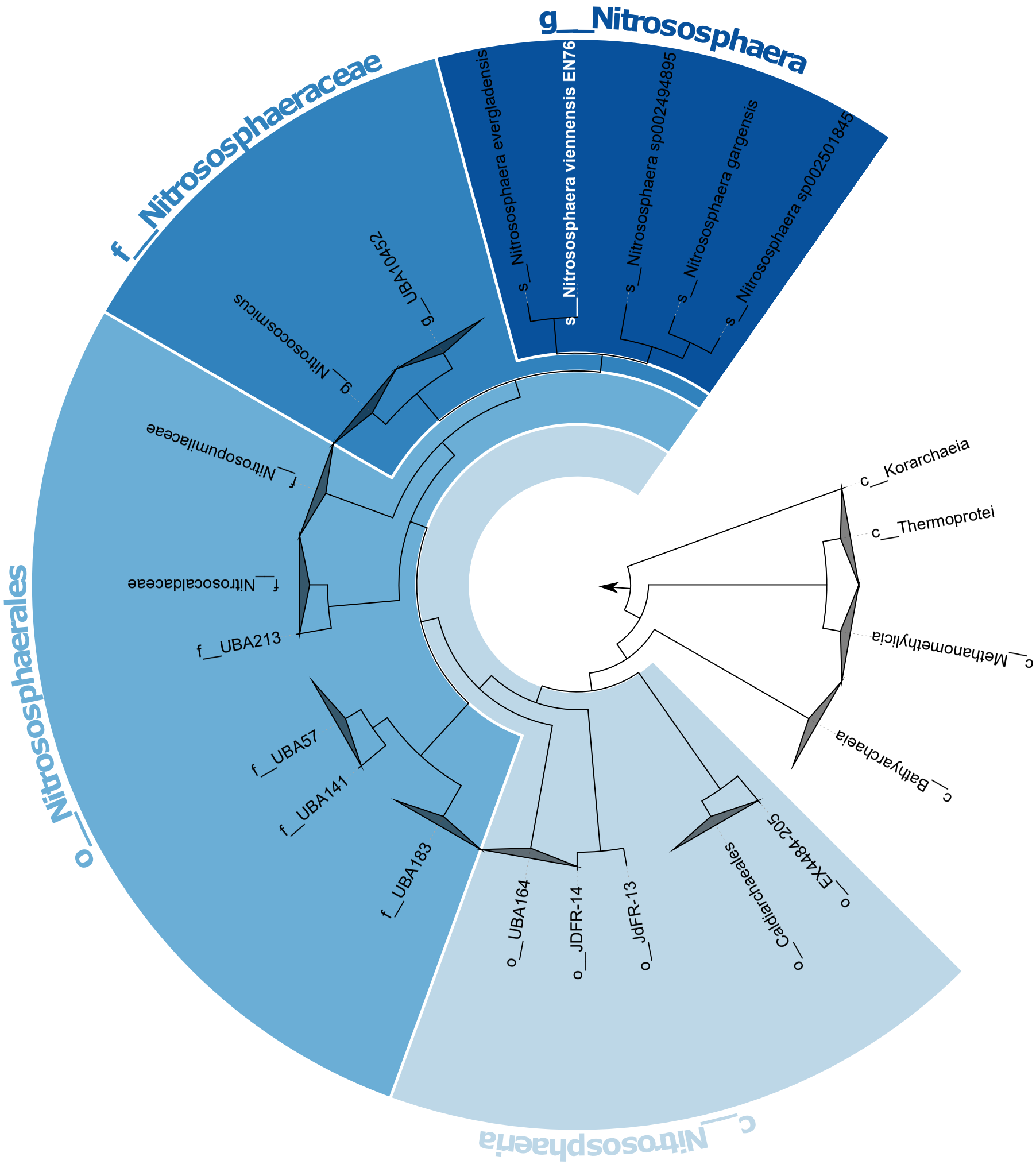
g__Nitrososphaera
s__Nitrososphaera evergladensis
s__Nitrososphaera viennensis EN76
s__Nitrososphaera sp002494895
s__Nitrososphaera gargensis
s__Nitrososphaera sp002501845
f__Nitrososphaeraceae
g__UBA10452
g__Nitrososcosmicus
f__Nitrosopumilaceae
f__Nitrosocaldaceae
f__UBA213
f__UBA57
f__UBA141
f__UBA183
o__Nitrososphaerales
o__UBA164
o__JDFR-14
o__JdFR-13
o__Caldiarchaeales
o__EX4484-205
c__Bathyarchaeia
c__Methanomethylicia
c__Thermoprotei
c__Korarchaeia
c__Nitrososphaeria